Origin of pulsar orthogonal polarization modes

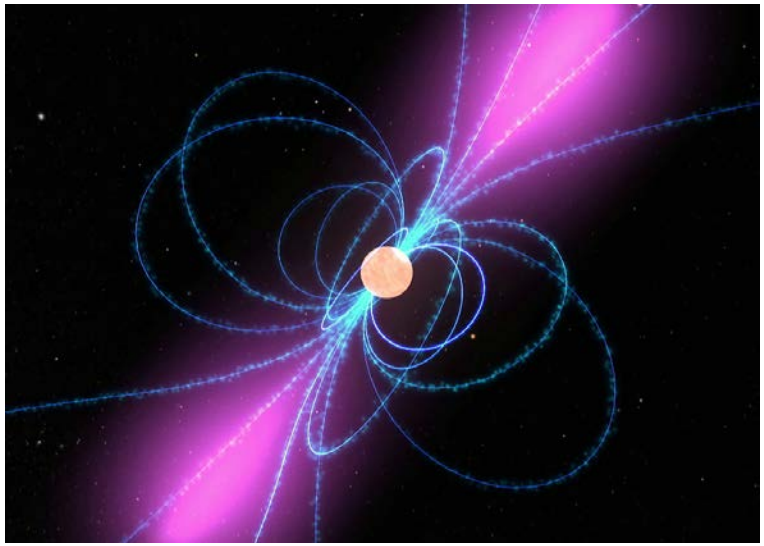

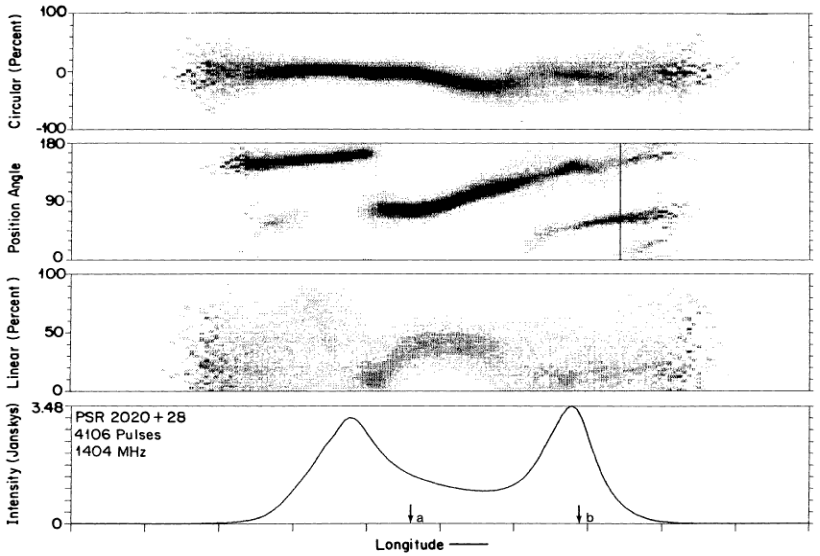

Chen WANG

P.F. WANG, Wei WANG, Jinlin HAN

National Astronomical Observatories, CAS

3rd US-Chinese Workshop, GBT, WV

Outline

- Polarized Curvature Radiation in Pulsar Magnetosphere (with both emission and propagation).

  => naturally generate orthogonal polarization modes (OPM)

  Wang, Wang & Han, 2014

- Distinguish orthogonal polarization modes of pulsar emission using spin axis and proper motion

  => constrain OPM model

  Wang 2014

Basic Physical Image of polarization evolution

Pulsar magnetosphere

1) Rotating dipole
2) ±e plasma streaming along B field line
3) Lorentz factor of the plasma γ ~ 400 ;
4) Density of the plasma

$$N_p = \eta N_{GJ}$$

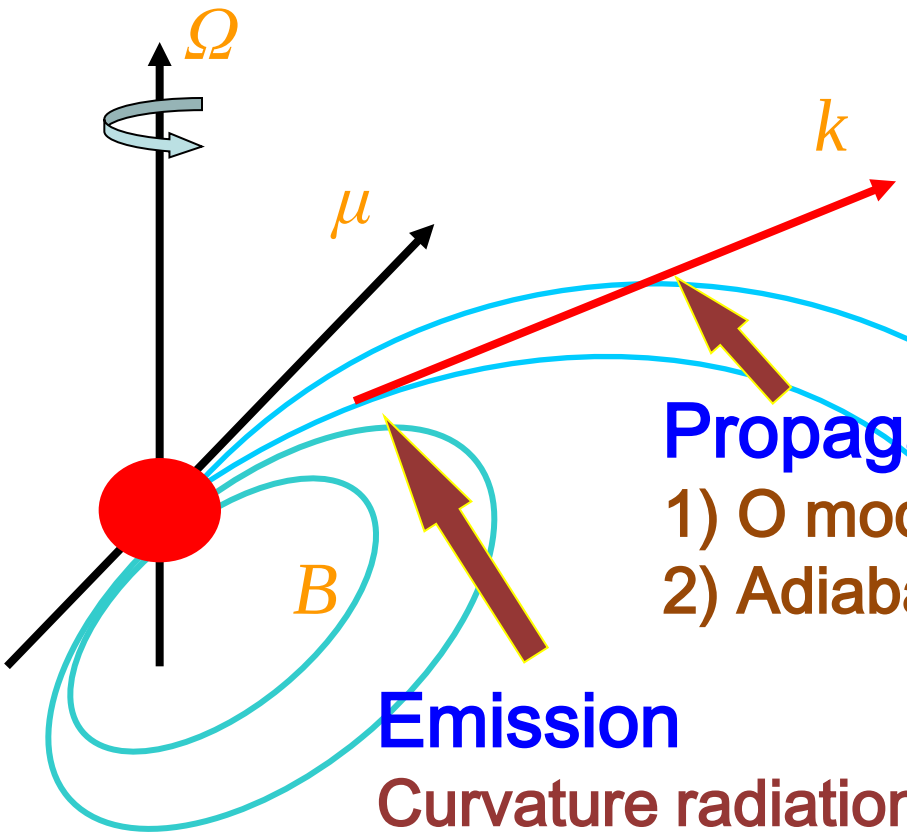

Propagation

1) O mode refraction
2) Adiabatic walking

Emission

Curvature radiation

Two linear eigenmodes of wave in pulsar magentosphere

Ordinary mode (O-mode), n < 1

Extraordinary mode (X-mode), n ~ 1

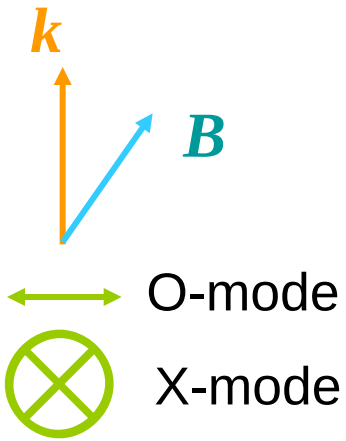

Refraction of O-mode wave

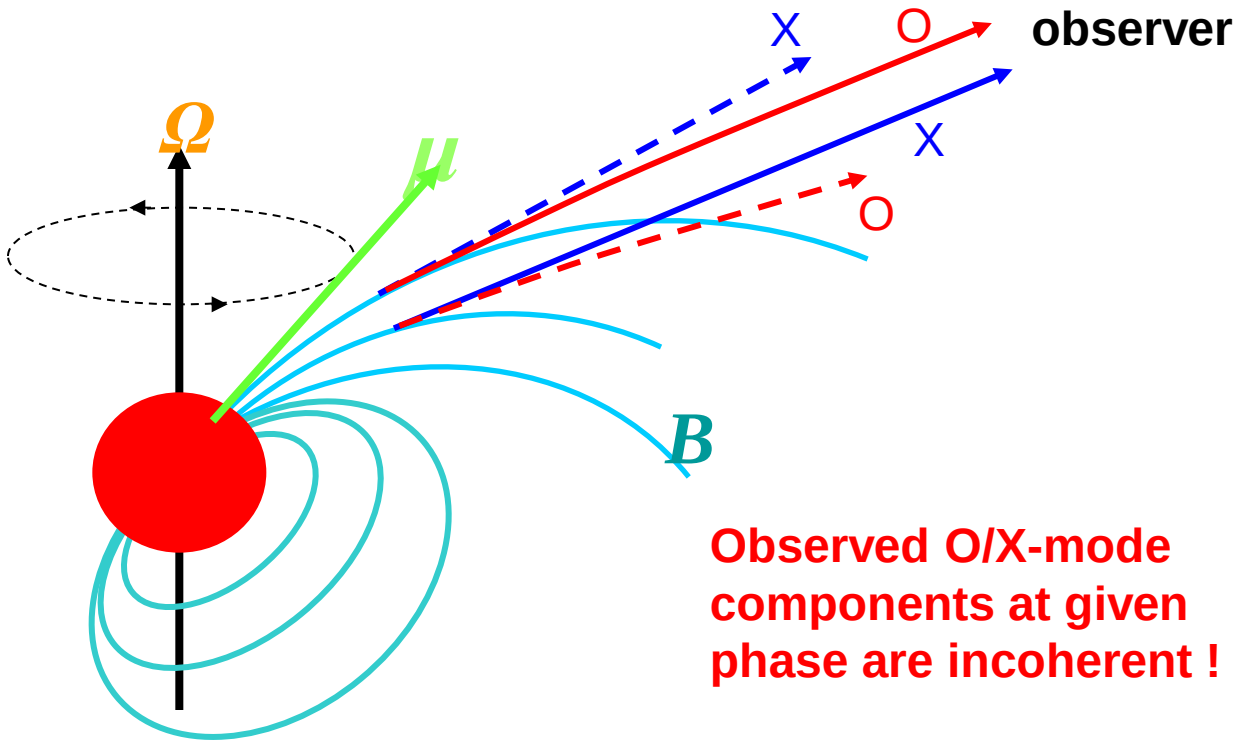

Observed O/X-mode components at given phase are incoherent !

The separation between the emission points of the O/X-mode waves

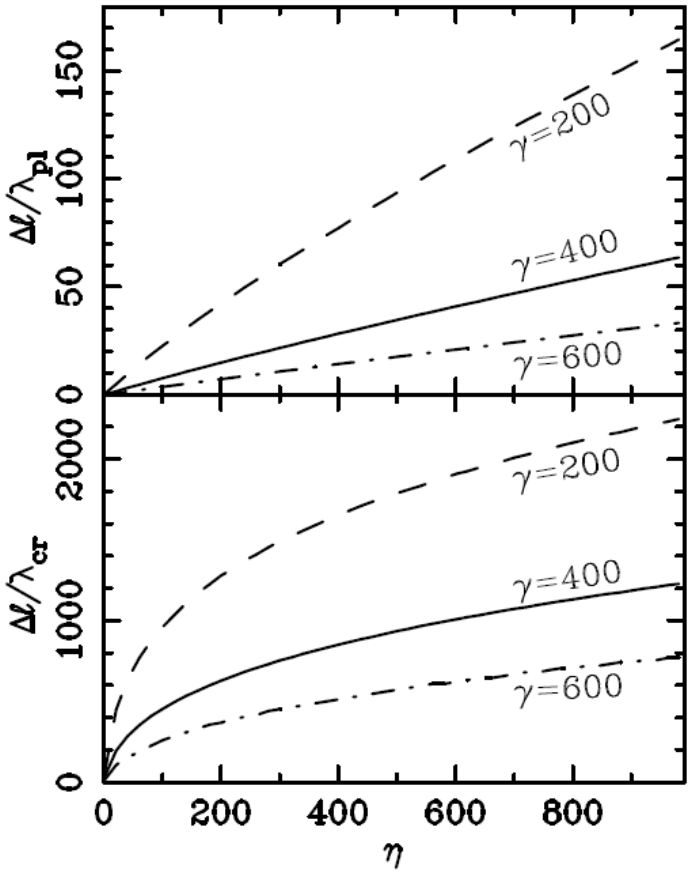

Curvature Radiation

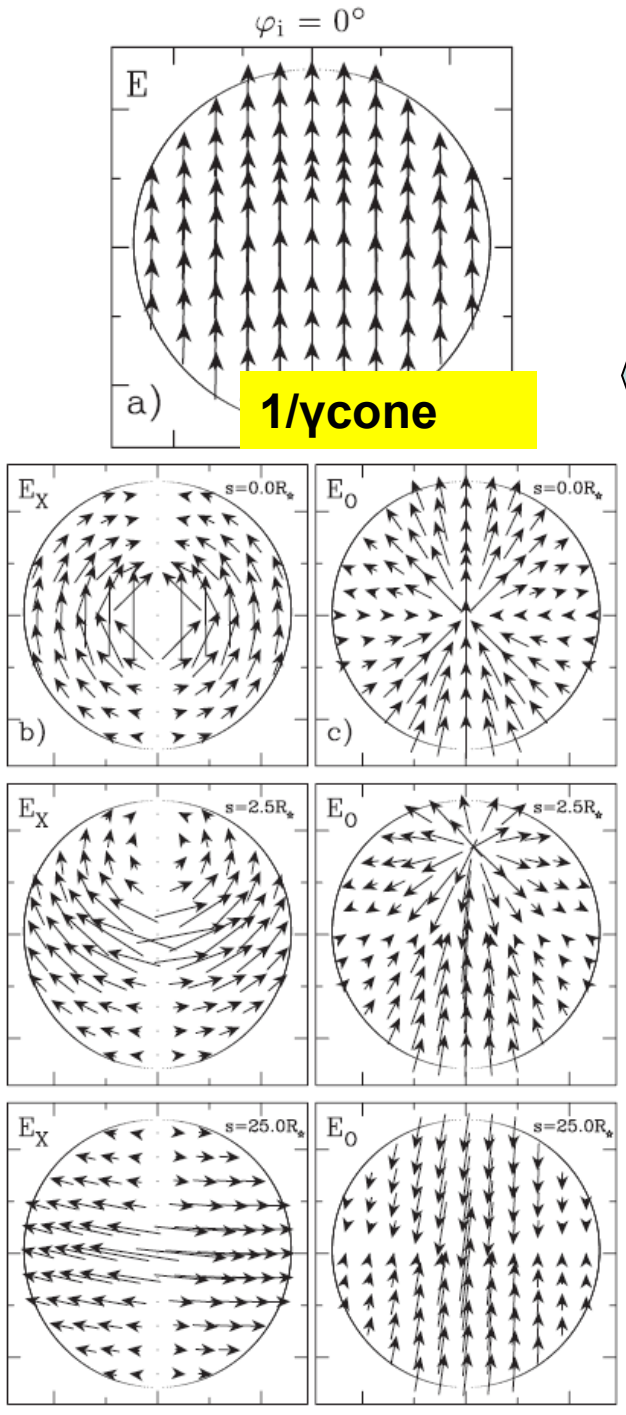

➢ **Without co-rotation**

V0 // B

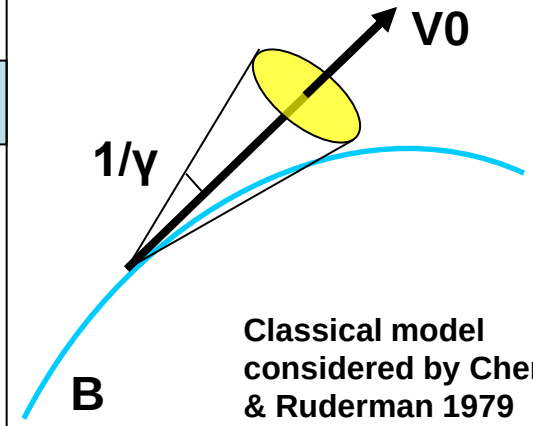

Classical model considered by Cheng & Ruderman 1979

➢ **With co-rotation**

V ∦ B

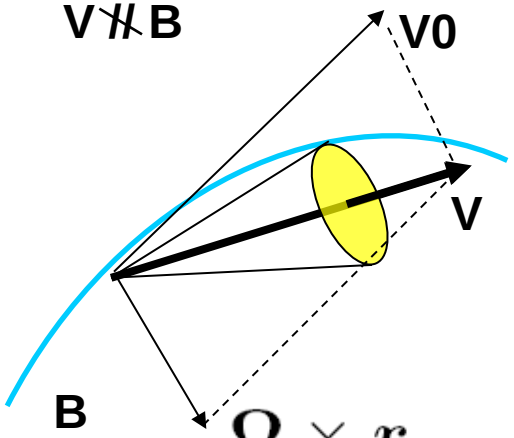

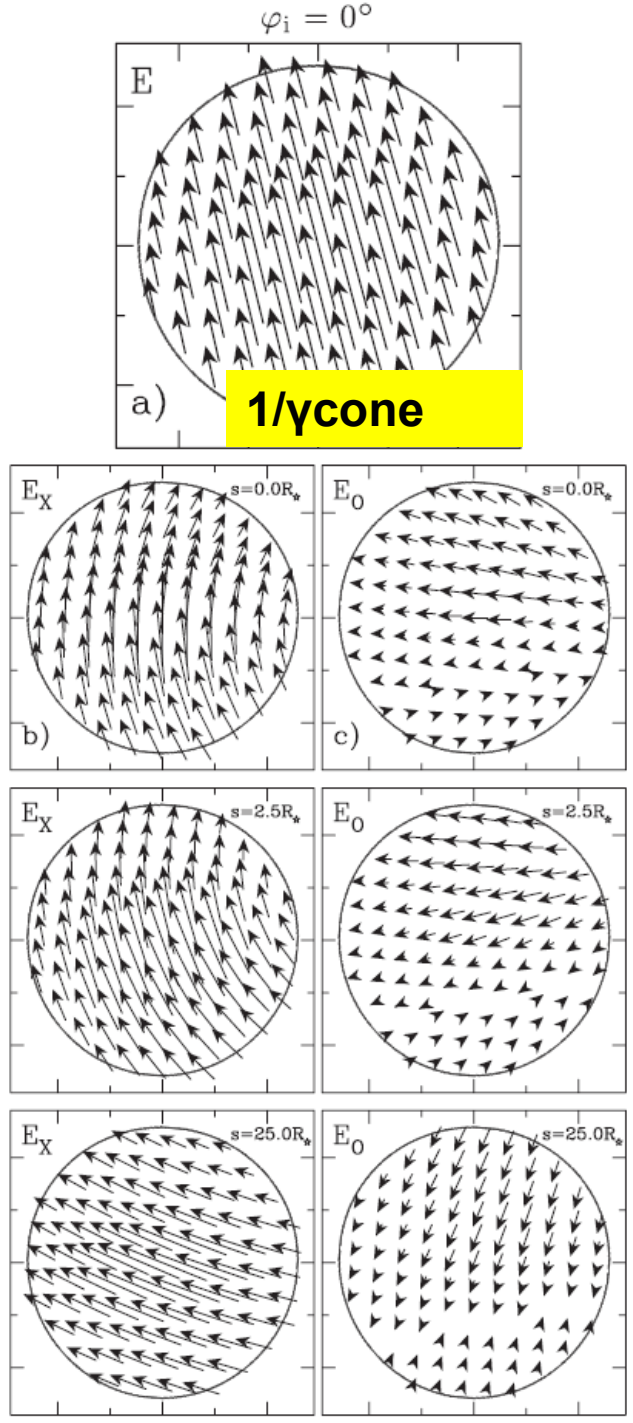

Without co-rotation

Emission beam

Uniform

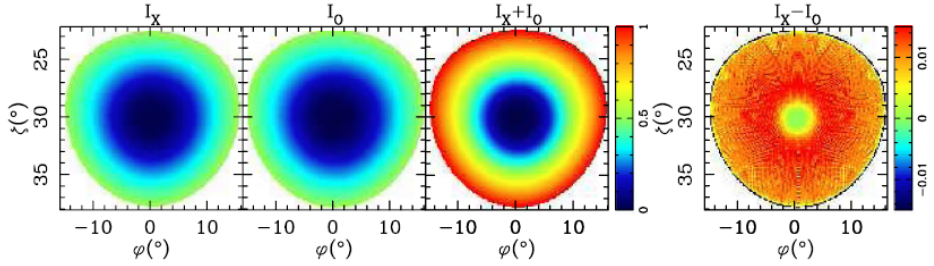

(a) Uniform density.

Cone

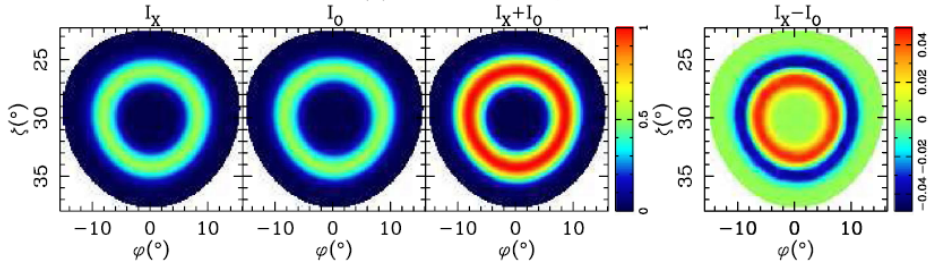

(b) Conal density.

Core

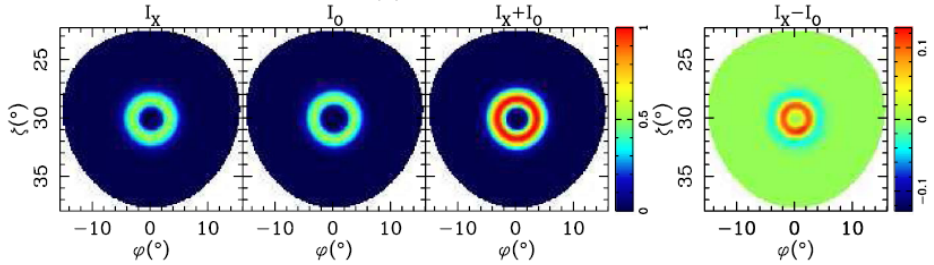

(c) Core density.

Patch

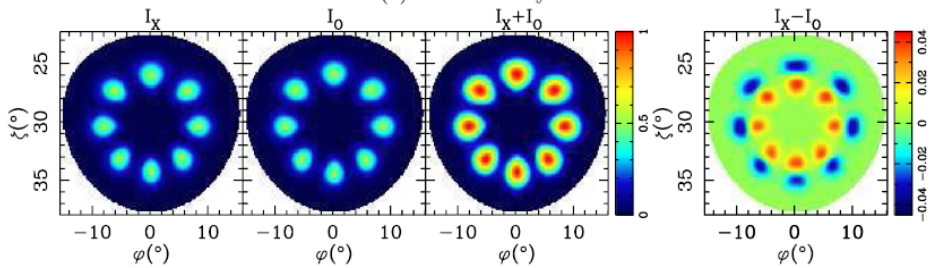

(d) Patch density.

Profiles with various impact angle

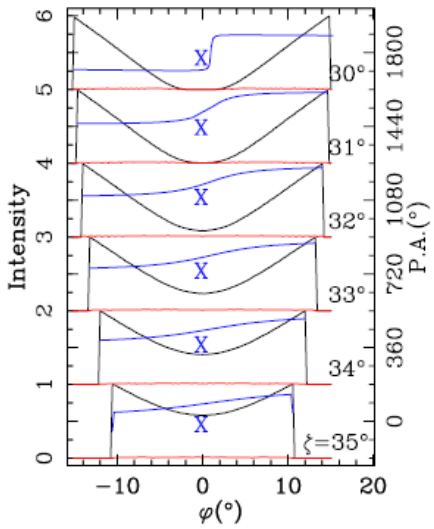

(a) Uniform density.

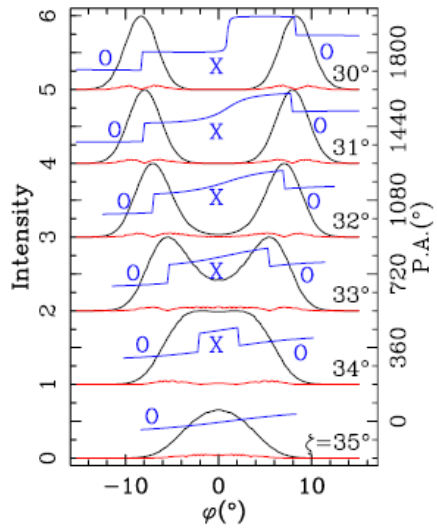

(b) Conal density.

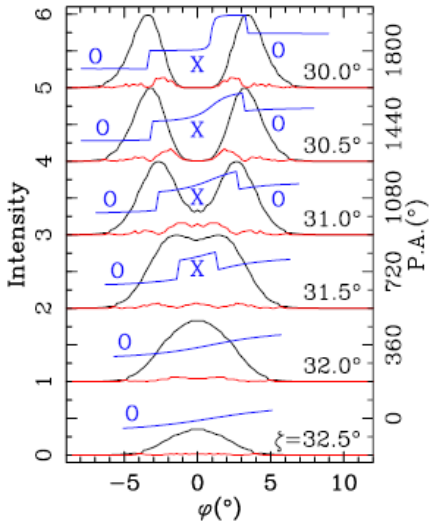

(c) Core density.

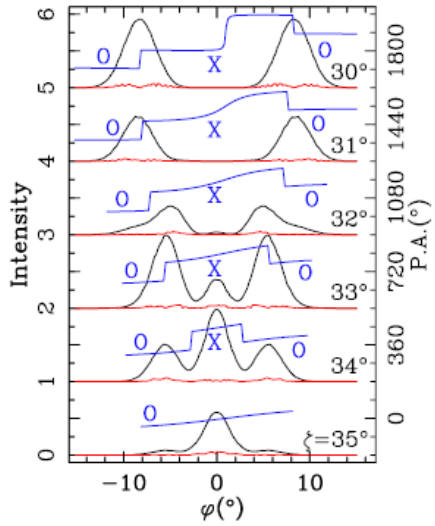

(d) Patch density.

With co-rotation

Emission beam

Uniform

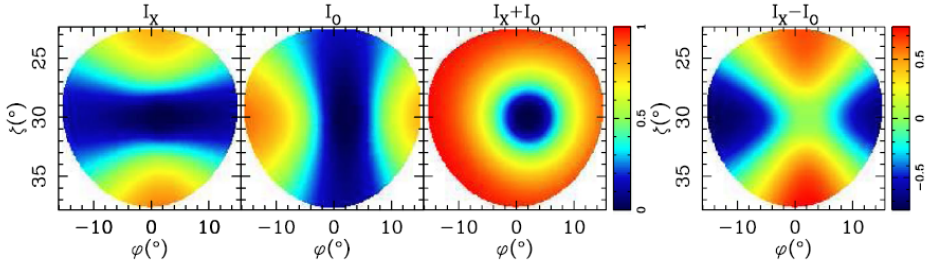

(a) Uniform density.

Cone

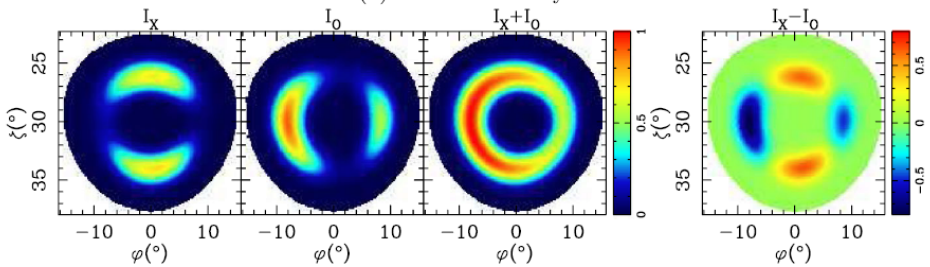

(b) Conal density.

Core

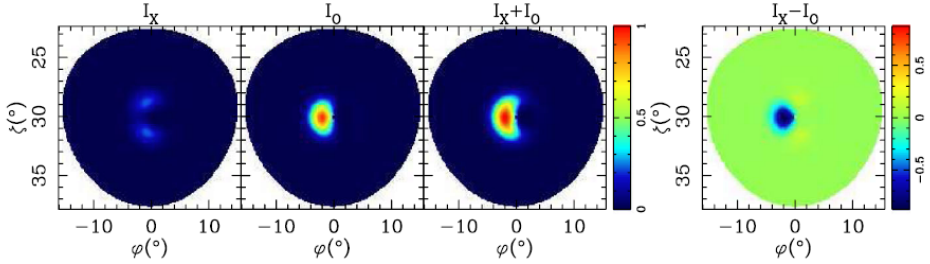

(c) Core density.

Patch

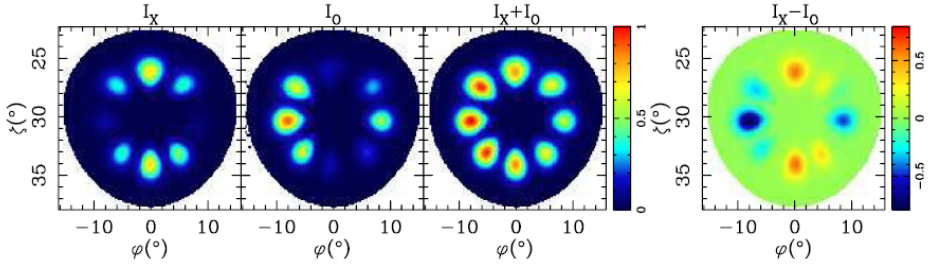

(d) Patch density.

Profiles with various impact angle

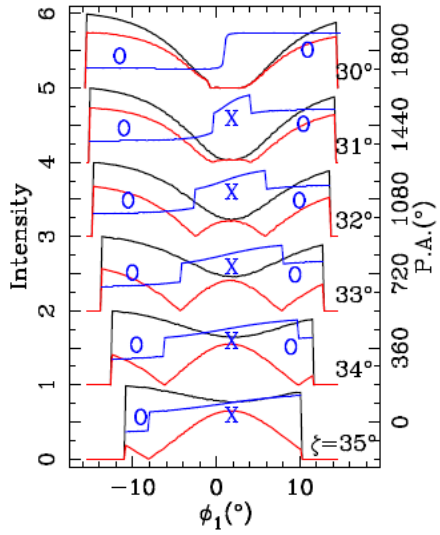

(a) Uniform density.

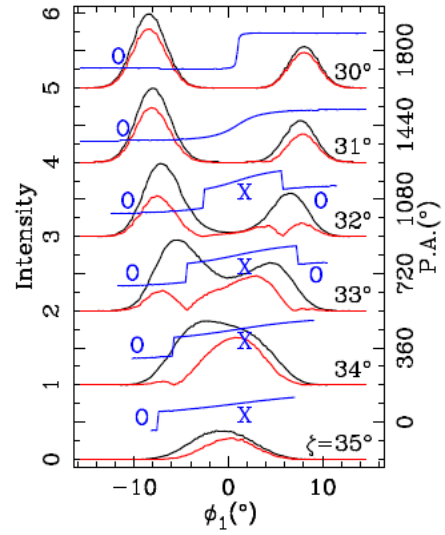

(b) Conal density.

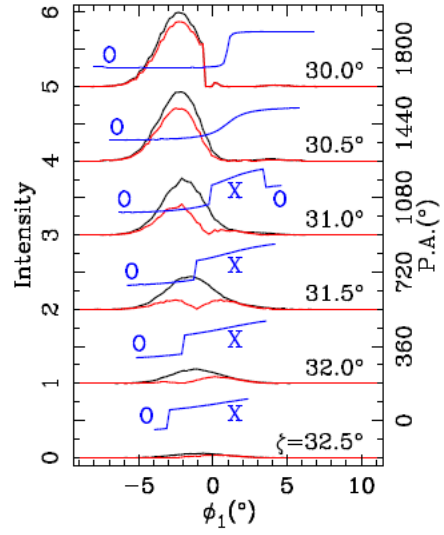

(c) Core density.

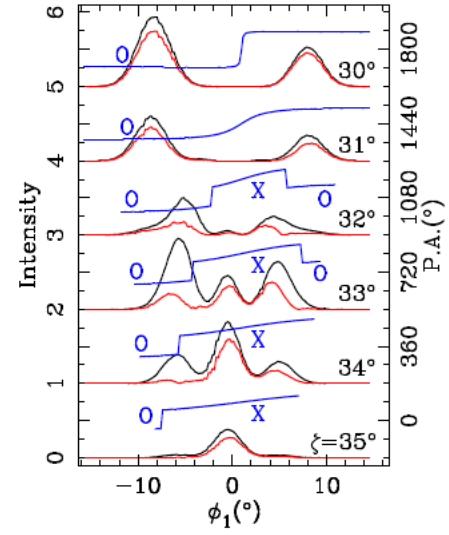

(d) Patch density.

Conclusion for polarized curvature radiation in pulsar magnetosphere

- The O-mode refraction separate X and O-mode components. which cause:
  - The observed X-mode and O-mode wave at given phase are emitted from incoherent region;
  - The orthogonal mode happens naturally due to the change of the dominance of the two modes;

- X/O-mode components of CR have:
  - almost the same magnitude without considering the co-rotation of plasma, which cause strong depolarization;
  - very different distribution with co-rotation included, high LP can be observed.

- Refraction induced OPM perfers “O X O” modes sequence. May be checked by observation!

Distinguish orthogonal polarization modes of pulsar emission

Orthogonal polarization mode for PSR B2020+28

Mean profile

Polarization of single pulses

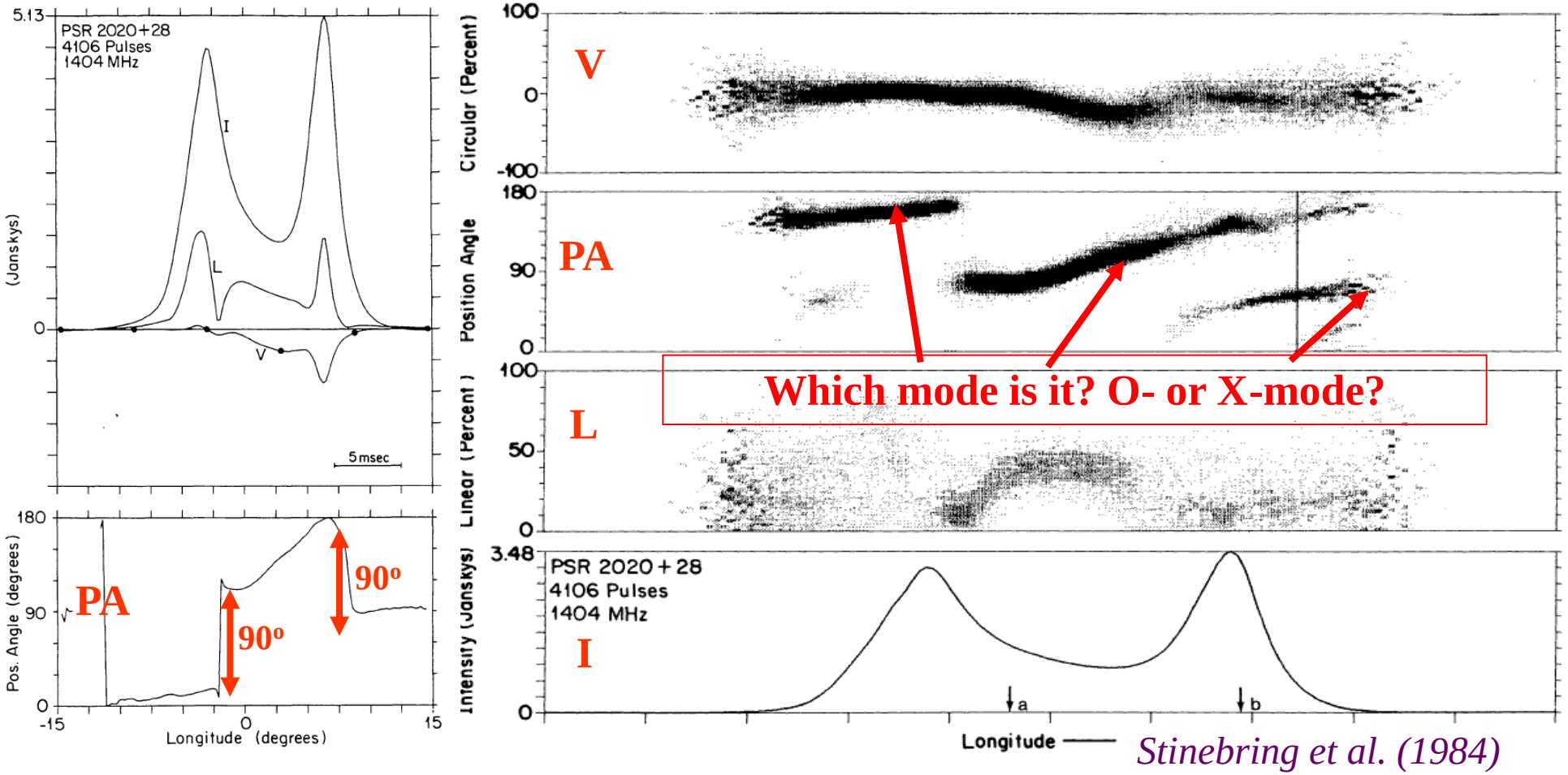

Stinebring et al. (1984)

Rotating Vector Model

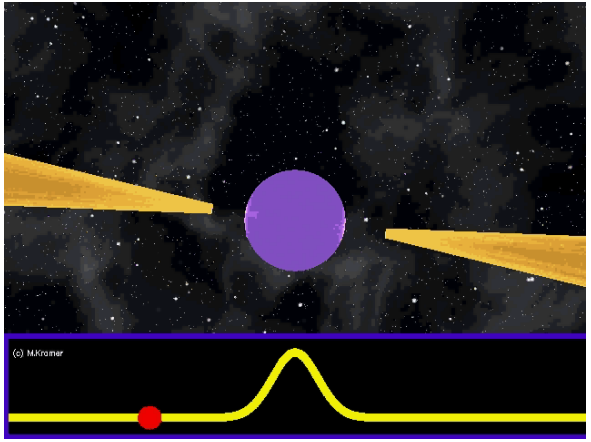

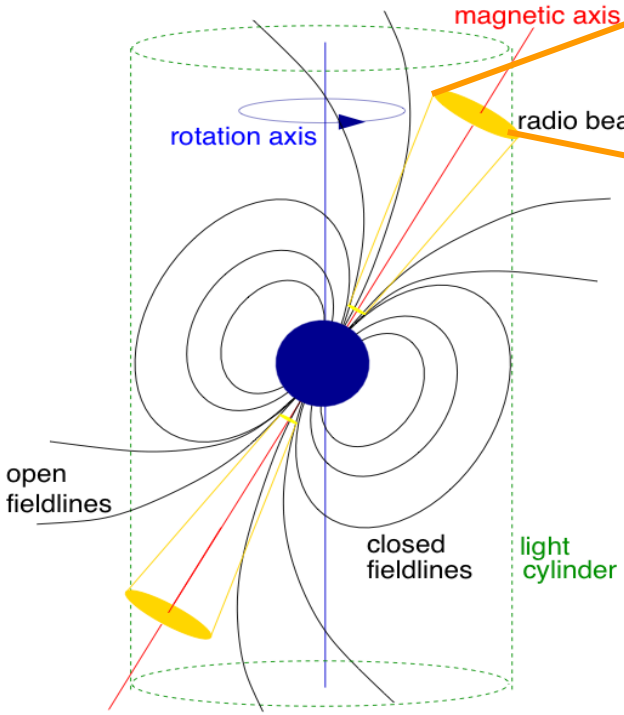

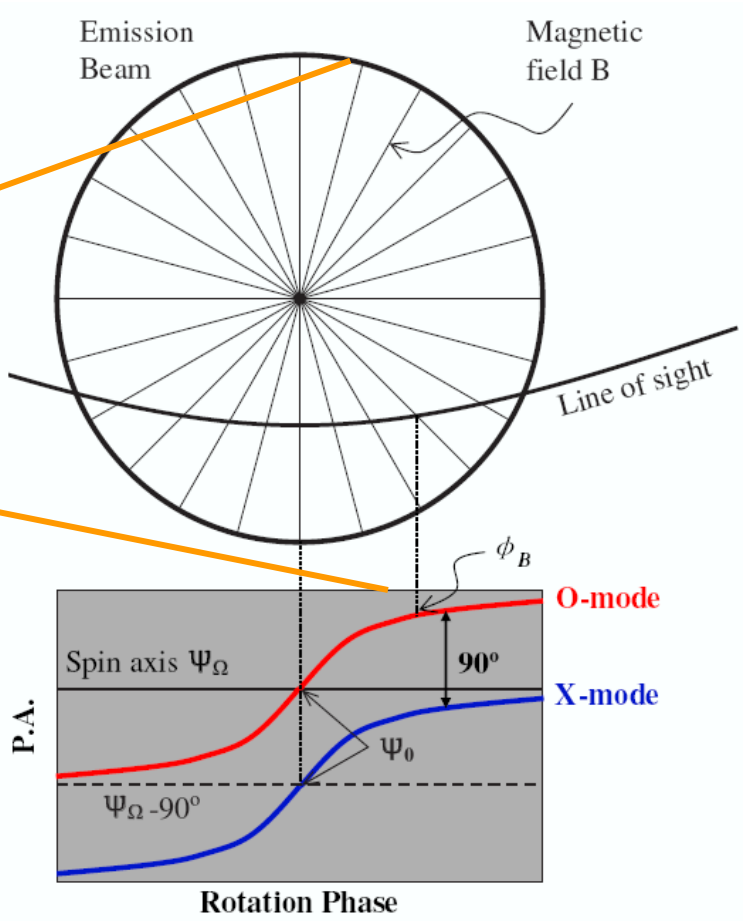

the angle difference $\Delta\Psi_{0\Omega} = \Psi_0 - \Psi_\Omega$
could be a criterion to distinguish the two wave modes.

$|\ \Delta\Psi_{0\Omega}\ | \sim 0^\circ$ ⟹ **O-mode**

$|\ \Delta\Psi_{0\Omega}\ | \sim 90^\circ$ ⟹ **X-mode**

Two ways to constrain spin axis Ψ_Ω

- Get spin axis directly by fitting the symmetric tori of PWNe around some young pulsars
  - obtain spin axis of 15 pulsars by Ng & Romani 2004, 2007, 2008.
  - Not avialable for normal pulsars without PWNe

- Using proper motion direction instead of spin axis according to spin-kick alignment
  - Spin-kick alignment proved by *Romani, Ng, Johnston, Wang, Noutsos et al.*
  - Proper motion measured by pulsar timing and interferometer obs. *Brisken et al. 2002, 2003; Hobbs et al. 2005.*

PWN of Vela: X-ray obs.

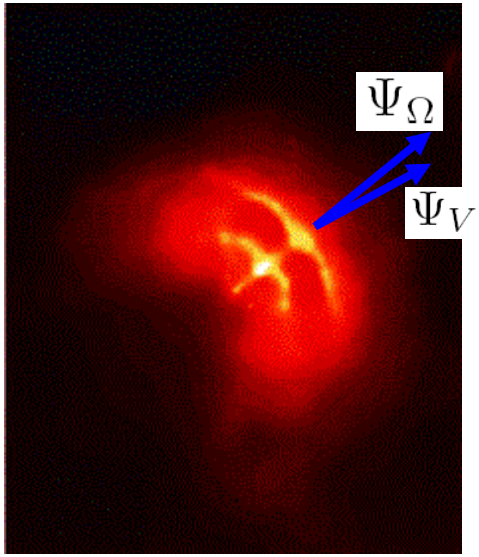

Ng & Romani 2004

Spin-kick alignment of pulsars

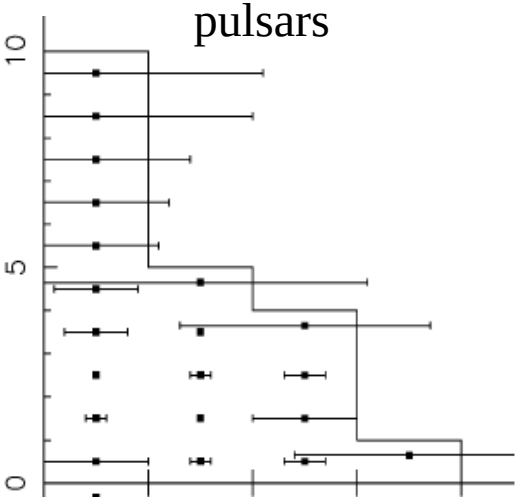

Noutsos et al. 2011

Mode distinguishment for 14 OPM-pulsars

(with both believable PM and PA data)

- For 7 pulsars, O-mode dominate central intensity-peak region. (X O X)
- For 4 pulsars, X-mode dominate intensity-peak region. (O X O)
- For 3 pulsars, each mode dominates half profiles

PSR	Ψ_V[a] deg	Ψ_0[a] deg	$\Delta\Psi_{0V}$ deg	Modes[b] L	P	T	Type[c]
OPM-pulsars with O-mode dominating intensity-peak region:							
J0452−1759	72(23)	47(3)	-25(23)	X	O		OPM
J0738−4042	-47(5)	-21(2)	26(5)	X	O	X	OPM
J1136+1551	-11.4(1)	-78(2)	-67(2)	X	O	X	OPM, CD
J1645−0317	-7(3)	56(4)	63(5)	X	O		OPM
J1709−1640	12(16)	15(2)	3(16)		O	X	OPM
J1932+1059	65.2(2)	-11.3(1)	-76.5(2)	X	O		OPM
J2022+2854	11(1)	12(10)	1(10)	X	O		OPM, CD
OPM-pulsars with X-mode dominating intensity-peak region:							
J0358+5413	69(16)	-33(5)	78(17)		X	O	OPM
J0953+0755	-4.1(2)	14.9(1)	19.0(2)	O	X	O	OPM
J1453−6413	37(3)	-56.9(4)	86(3)	O	X	O	OPM
J1820−0427	-22(17)	42(3)	64(17)	O	X		OPM
OPM-pulsars with the two mode dividing profiles equally:							
J1239+2453	-65.0(1)	-66(1)	-1(1)	X		O	OPM
J1900−2600	22.8(7)	-43(2)	-66(2)	X		O	OPM
J2018+2839	23(2)	89(20)	66(20)	X		O	OPM
OPM-pulsar hard to distinguish modes:							
J1913−0440	-14(11)	-68(2)	-54(11)	unknown			OPM

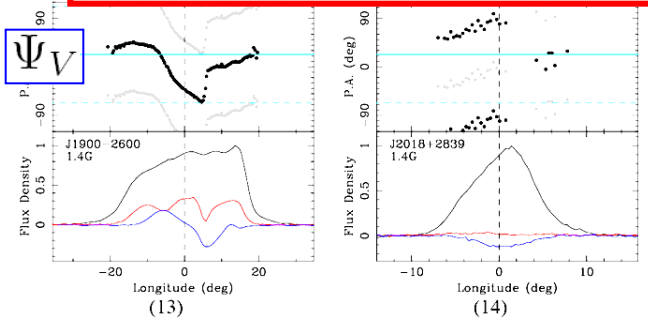

Polarization profiles comes from Johnston et al. 2005, 2007; Carr 2007; Han et al. 2009

Possible constrains on origin of OPM

- Refraction effect. O-X-O (4 pulsars)
  - O mode refracted towards away from magnetic axis.

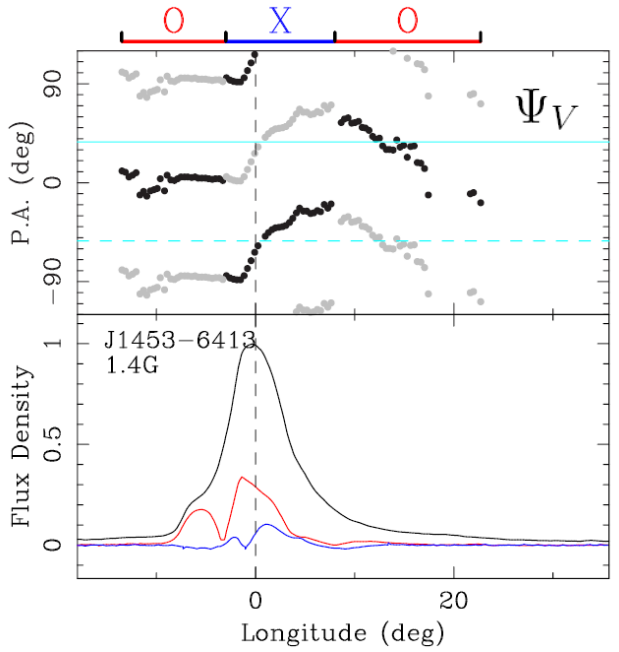

- Emission mechanism origin. Cheng & Ruderman 1979, X-O-X (7 pulsars)
  - Central O-mode emission from parallel accelaration
  - X-mode from curvature radiation dominates two wings

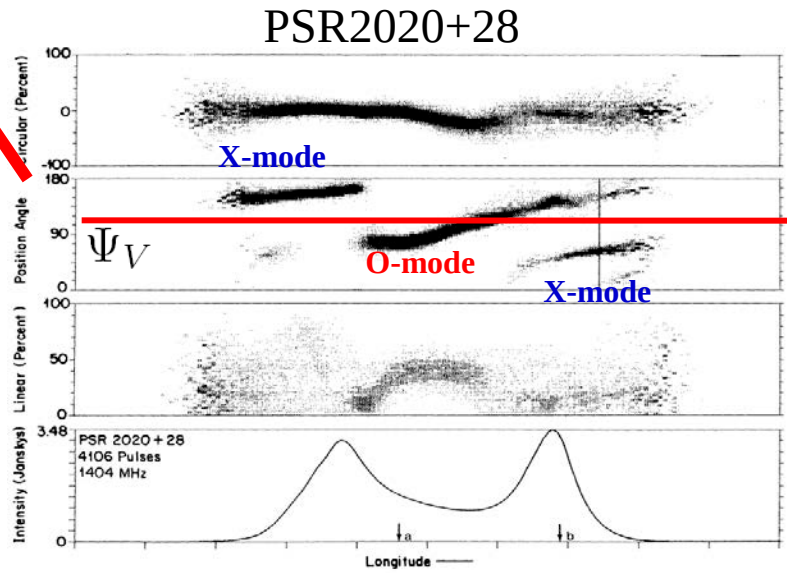

- Different OPM-pulsars may have different origin of OPM.

Summary

- Refraction of O-mode seperates the two eigenmodes and make them incoherent, which naturally causes OPM.

- X/O-mode components of curvature radiation have:
  - almost the same magnitude without considering the co-rotation of plasma, which cause strong depolarization;
  - very different distribution with co-rotation included, high LP can be observed.

- Modes sequence of OPM perfer “O X O”

- Polarization modes of 14 OPM-pulsars can be recognized by pulsar spin axis and/or proper motion.
  - 4 of them agree with “O X O” modes sequence
  - 7 of them are “X O X”, 3 of them are “X O”.
  - Different OPM-pulsars may have different origin of OPM.

年轻脉冲星星风云X-ray观测

部分PWN为环状结构

可以直接确定自转轴方向

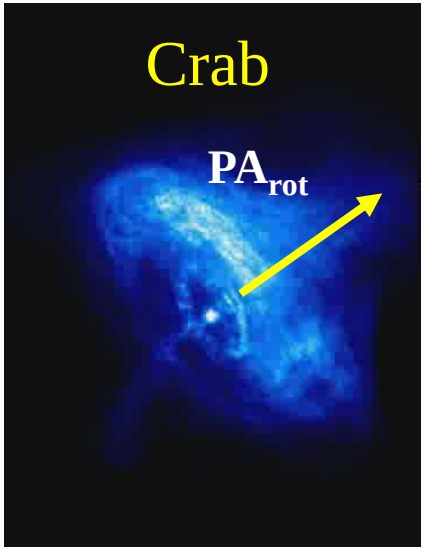

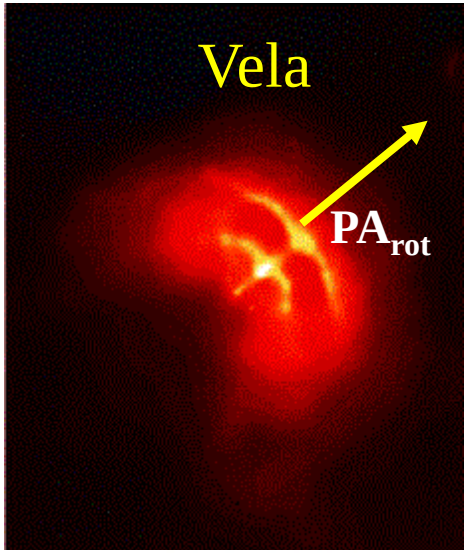

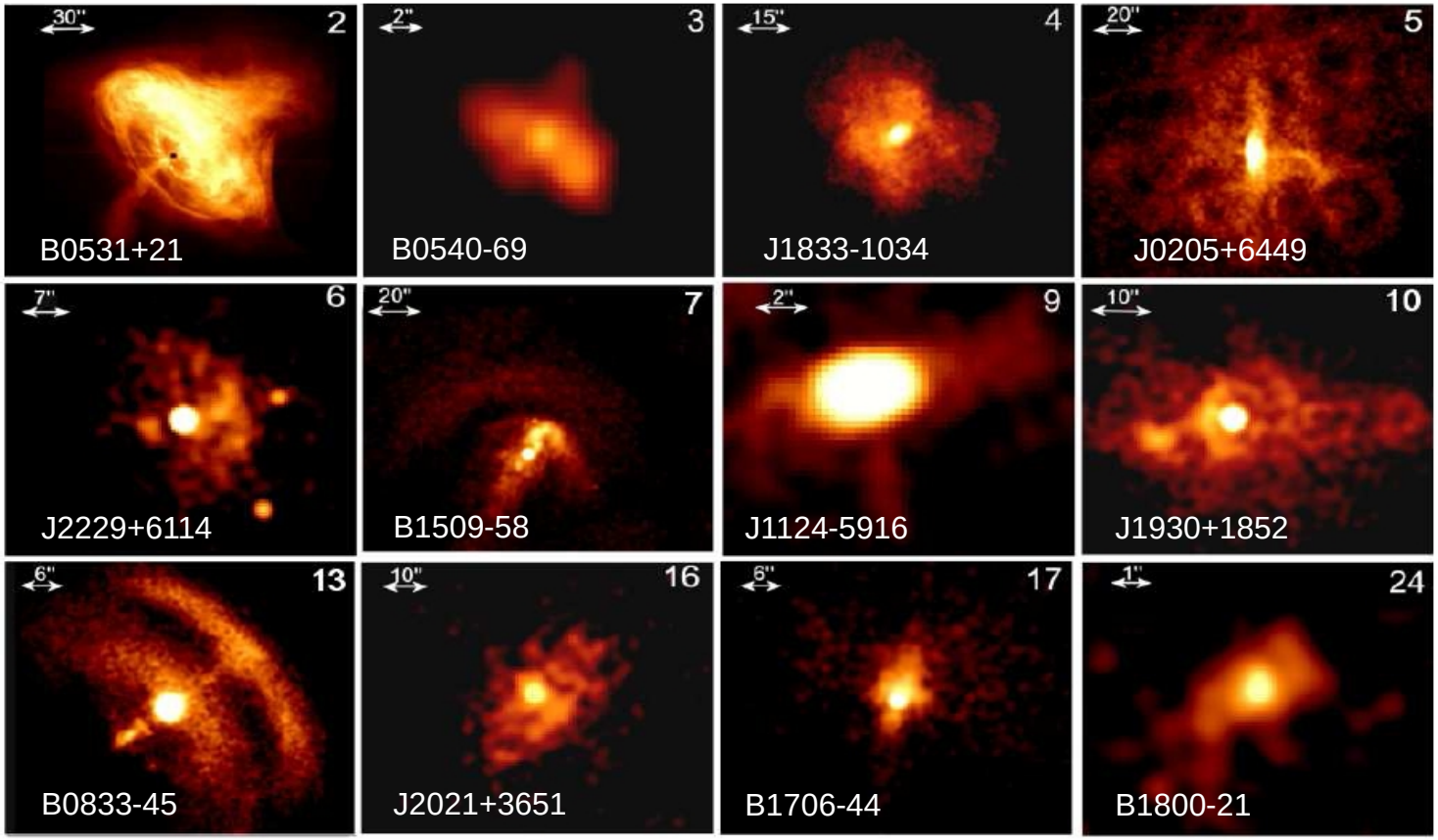

Kargaltsev & Pavlov 2008

Mode distinguishment for 3 young pulsars

Both spin axis and well-calibrated polarization position angle curve is needed

PSR	Ψ_Ω[a] deg	Ψ_0[b] deg	$\Delta\Psi_{0\Omega}$ deg	Ψ_V[b] deg	$\Delta\Psi_{\Omega V}$ deg	$\Delta\Psi_{0V}$ deg	Modes
J0538+2817	155(8)	-49(10)	-24(13)	-24.1(2)	-1(8)	-25(10)	O
J0835-4510	130.6(12)	36.8(1)	86.2(12)	301.0(1)	9.6(12)	-84.2(1)	X
J1709-4429	163.6(23)	72(10)	88(10)	160(10)	4(10)	-88(14)	X

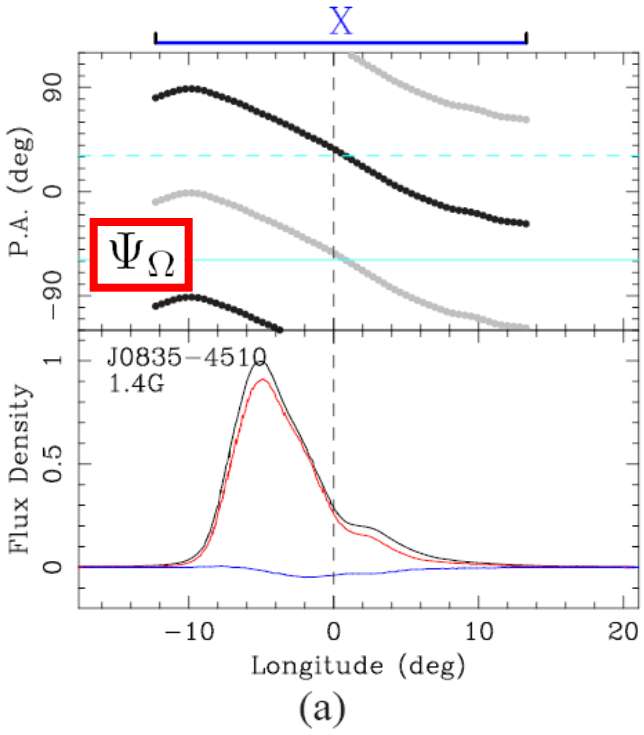

(a)

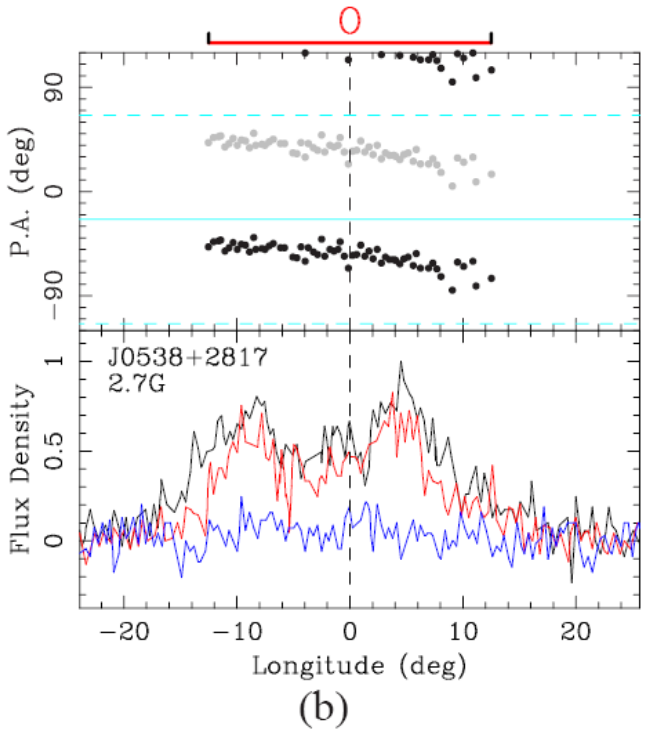

(b)

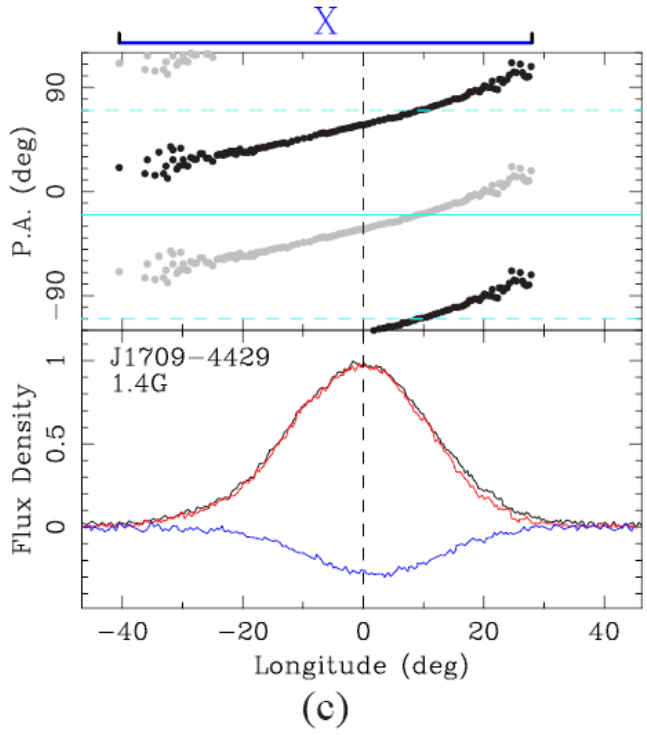

(c)

普通脉冲星：spin-kick趋于一致

利用偏振曲线最陡处PA_0代替spin，统计PA_{0v}的分布

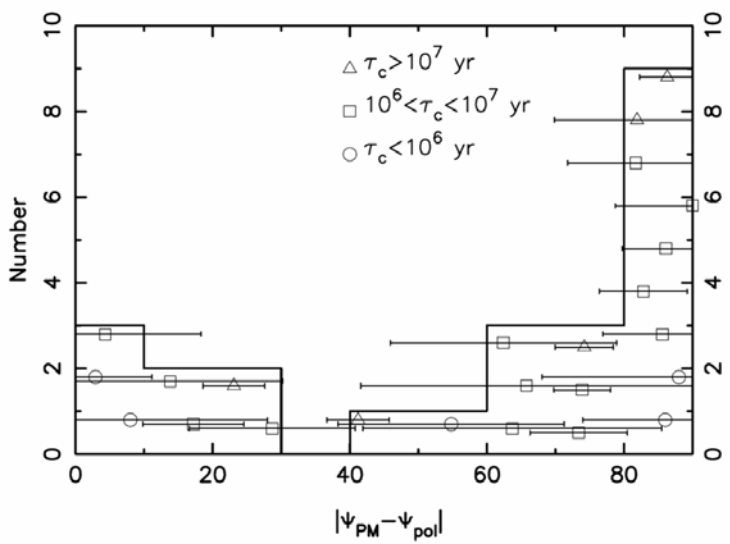

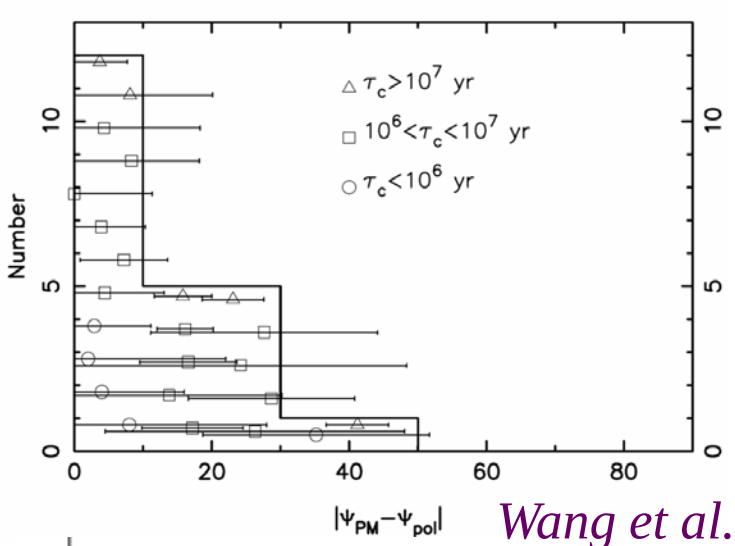

Wang et al. 2006

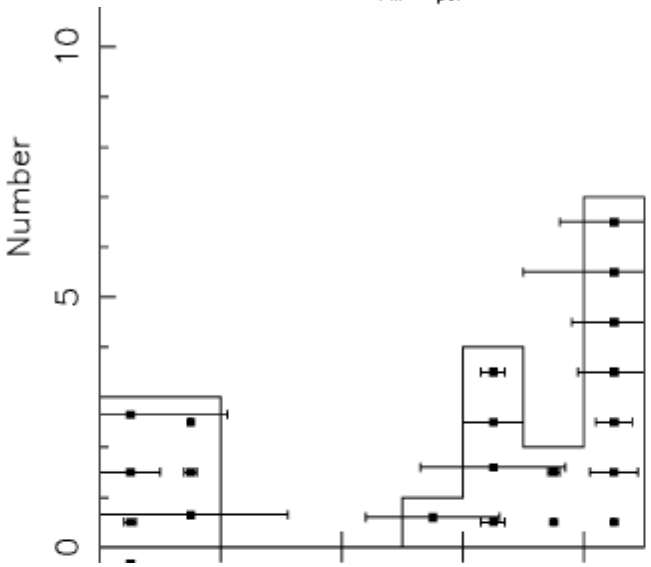

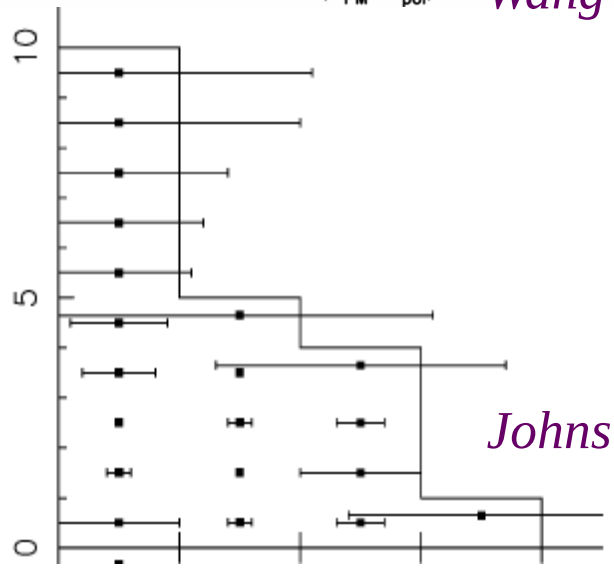

Johnston et al. 2005

讨论

- 利用自行与PA最陡处偏振位置角之差（PA_{0v}）辨别模式的前提：
  - Spin-kick趋于一致。是否可靠？
    - 年老的脉冲星可能不一致
    - 部分年轻或正常脉冲星也有可能不一致。
  - 传播效应对PA曲线垂直方向影响不大。基本可靠!
  - 确定PA曲线最陡处的位置。对基本符合RVM描述的S型比较容易。但是对S曲线不完整的比较勉强！

- 下一步工作：获得更大的PA_{0v}样本。
  - 偏振观测与校准
  - 多波段偏振观测
  - 自行观测数据，长期timing或者VLBI观测获得。

- 下一步工作：正交模式的起源。正在进行中...

总结

- 利用年轻脉冲星星风云X-ray观测得到的自转轴方向可以辨别偏振模式，但是个数太少。
- 根据spin-kick的一致性，可以利用自行方位与PA最陡处偏振位置角之差（PA_{0V}）来辨别偏振模式
  - PA_{0V}~ 0 ^{o} 为O-mode
  - PA_{0V}~ 90 ^{o}为X-mode
- 应用：
  - 利用PA_{0V}辨别了12颗脉冲星的正交模式，发现
    - 8颗脉冲星 X-mode位于leading side
    - 4颗脉冲星 O-mode位于leading side
  - 利用PA_{0V}辨别了4颗conal-double PSRs 的偏振模式，有3颗是O-mode。
- 需要更多的校准好的偏振数据以及自行数据进行下一步统计研究。

Cheng & Ruderman 1979

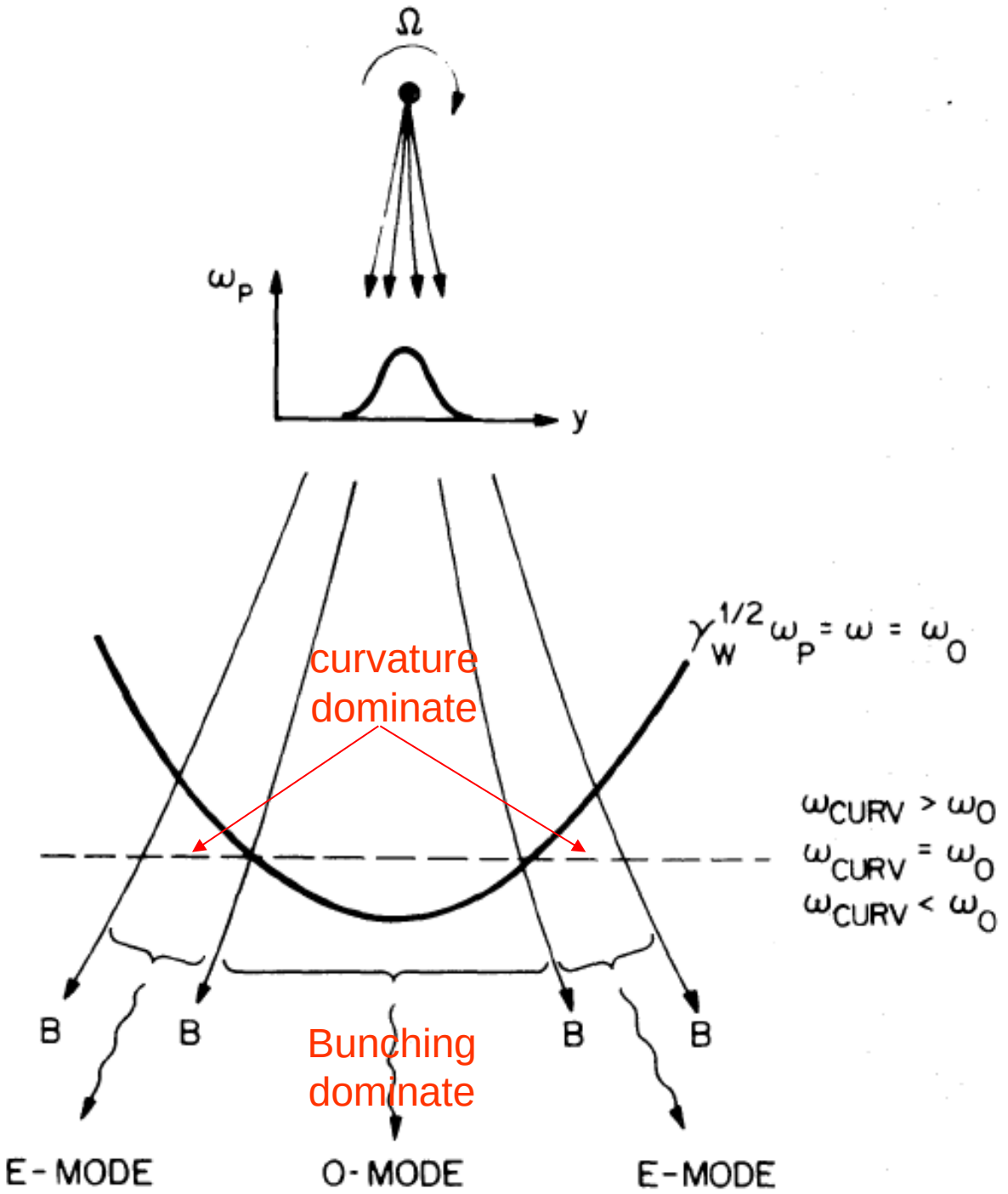

星风云的详细结构

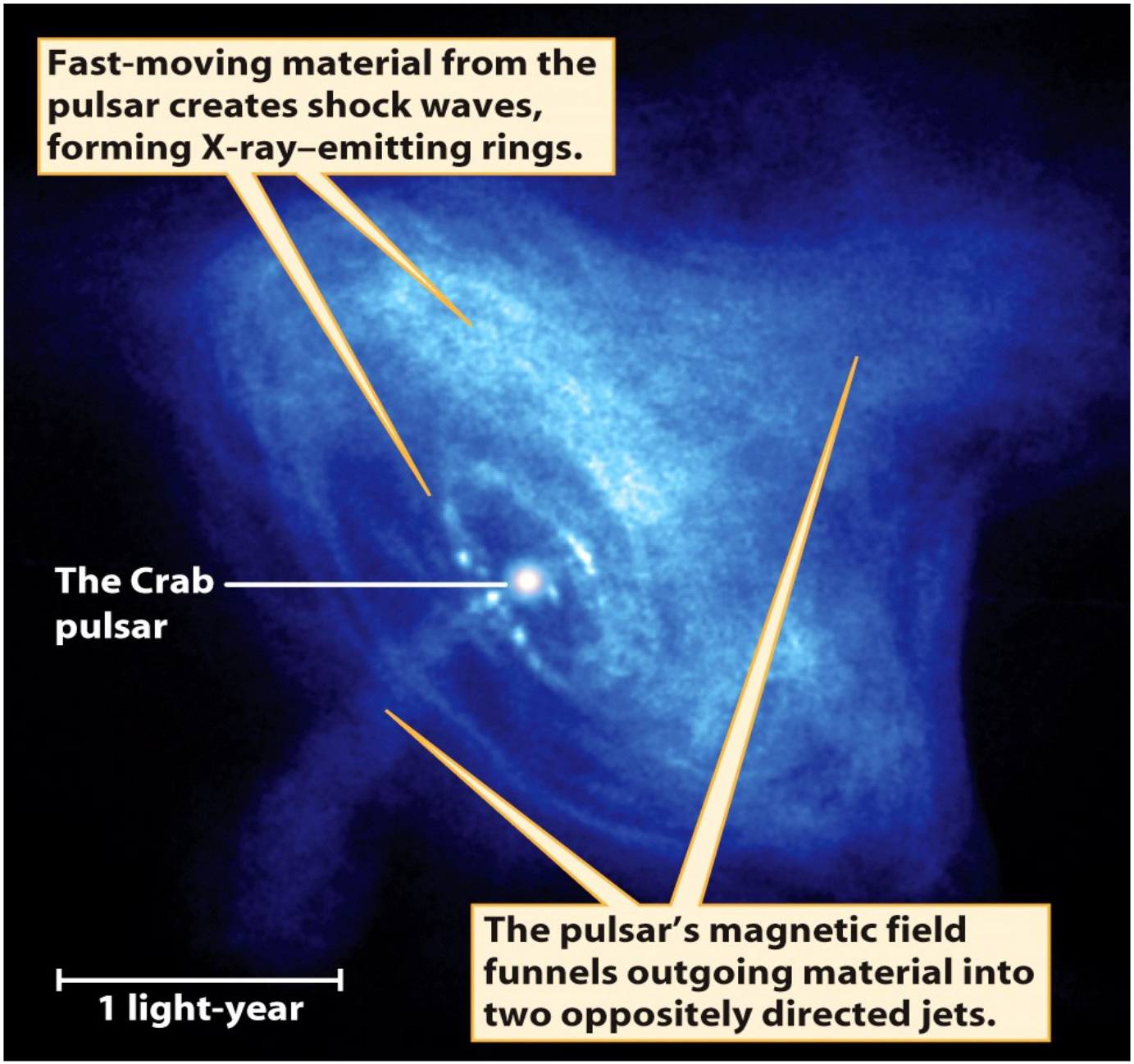
Fast-moving material from the pulsar creates shock waves, forming X-ray–emitting rings.
The Crab pulsar
1 light-year
The pulsar's magnetic field funnels outgoing material into two oppositely directed jets.

Vela 脉冲星星风云的结构

G. G. Pavlov et. al. ApJ. 591:1157

C.-Y. Ng ApJ.601:479 (FITTING PWN TORI)

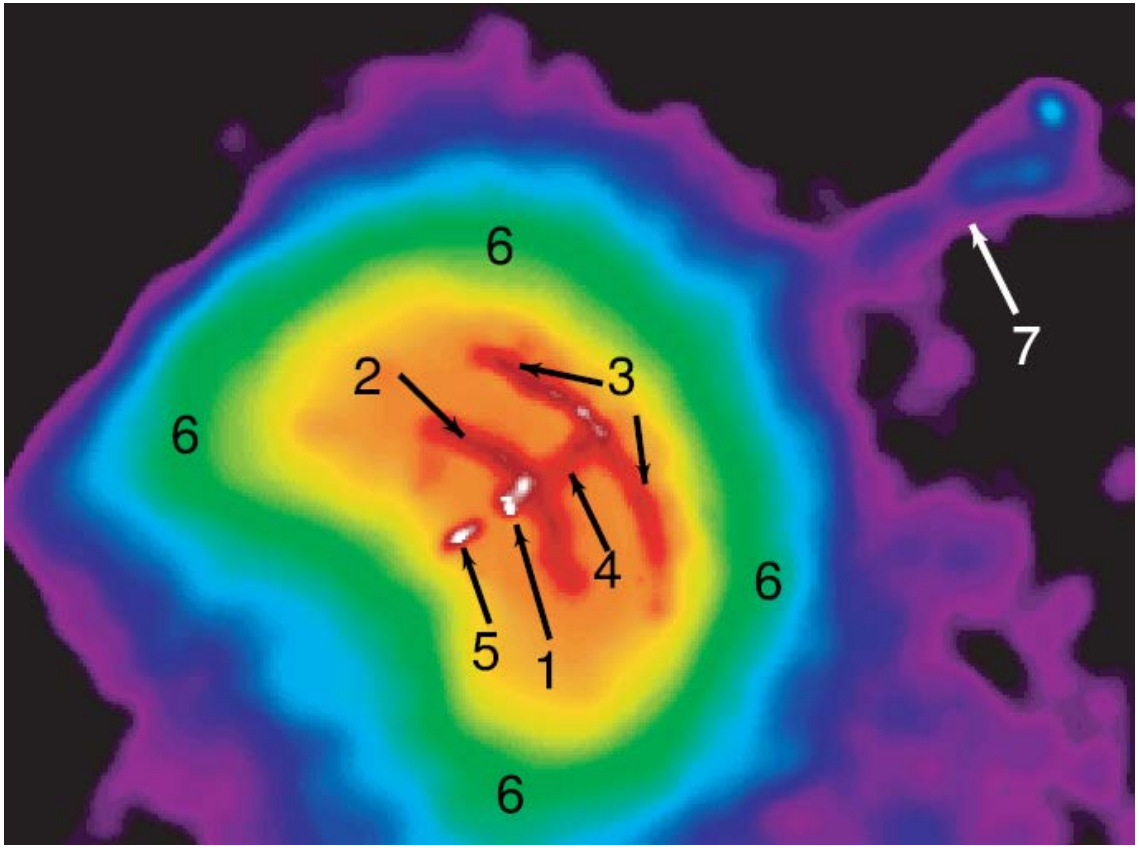

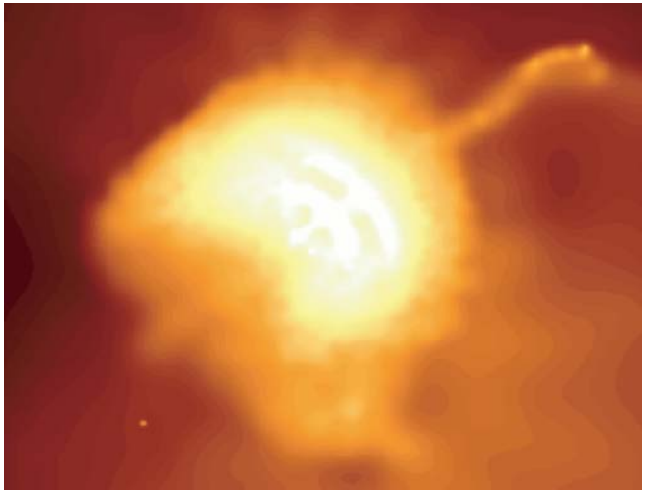

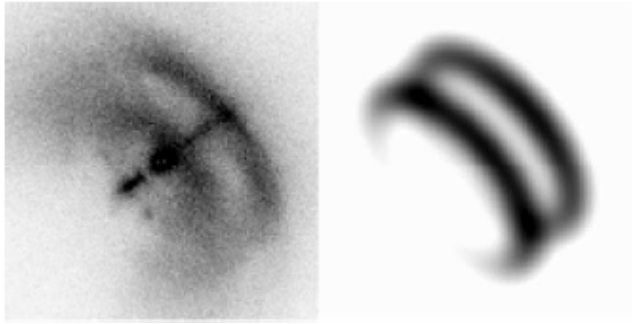

Chandra ACIS-S3 image of Vela PWN : (1) Vela pulsar, (2) inner arc, (3) outer arc, (4) inner jet, (5) counter jet, (6) shell, (7) outer jet.

考虑spin-kick的一致性，可以用自行代替自转轴方向
判断自行方向角PA_v与PA最陡处PA_0的差值PA_{0v}

- $PA_{0v} \sim 0^o$ => O-mode
- $PA_{0v} \sim 90^o$ => X-mode

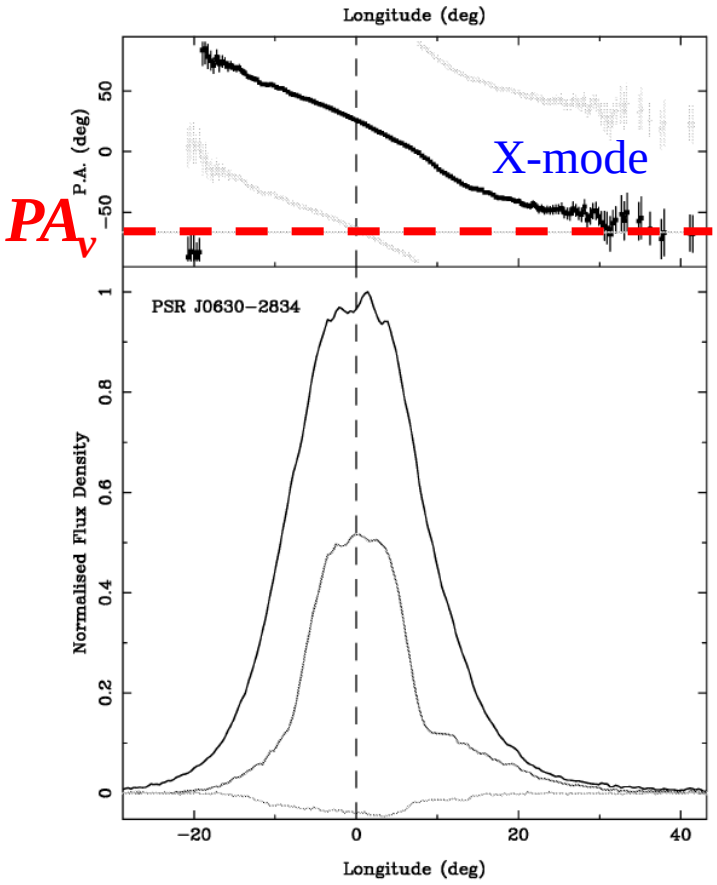

Two Vela-like PSRs

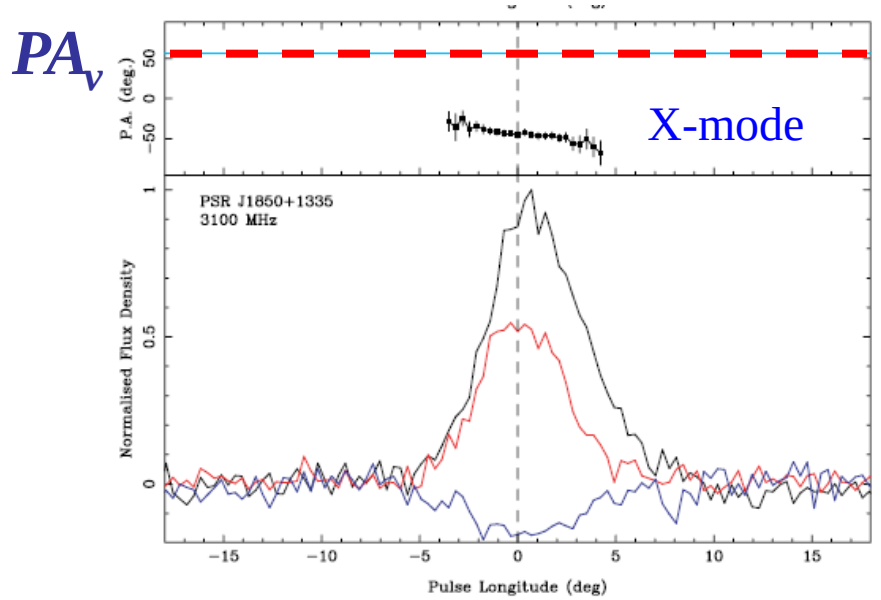

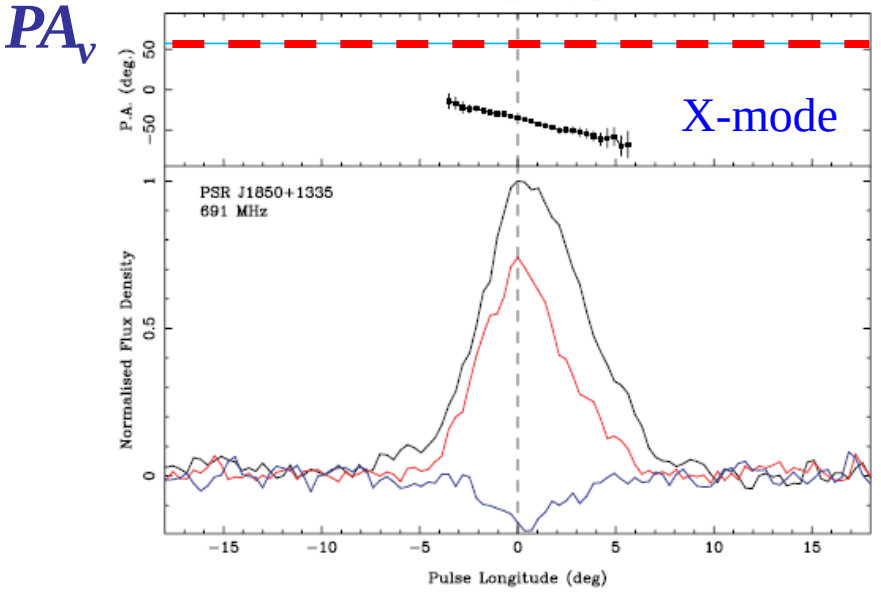

应用PA_{0v}辨别正交模式

B1929+10

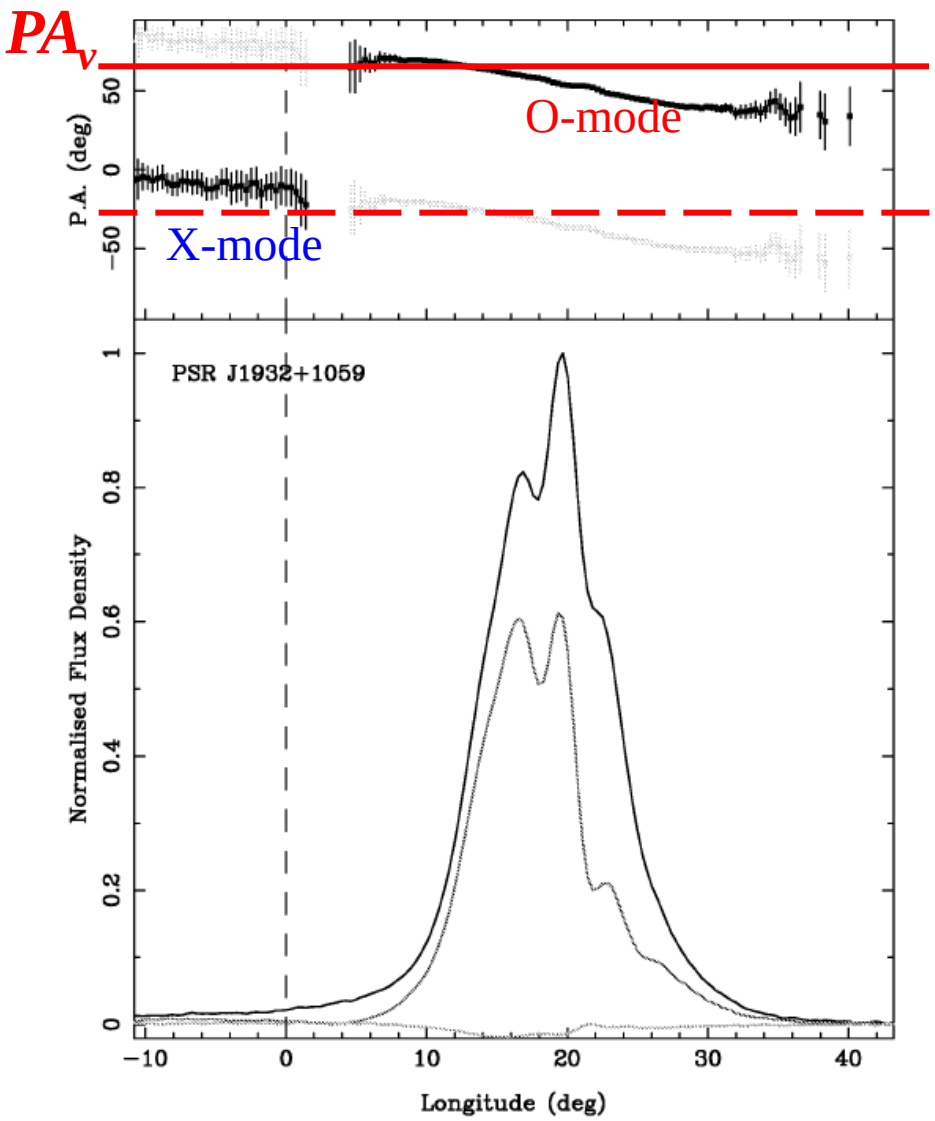

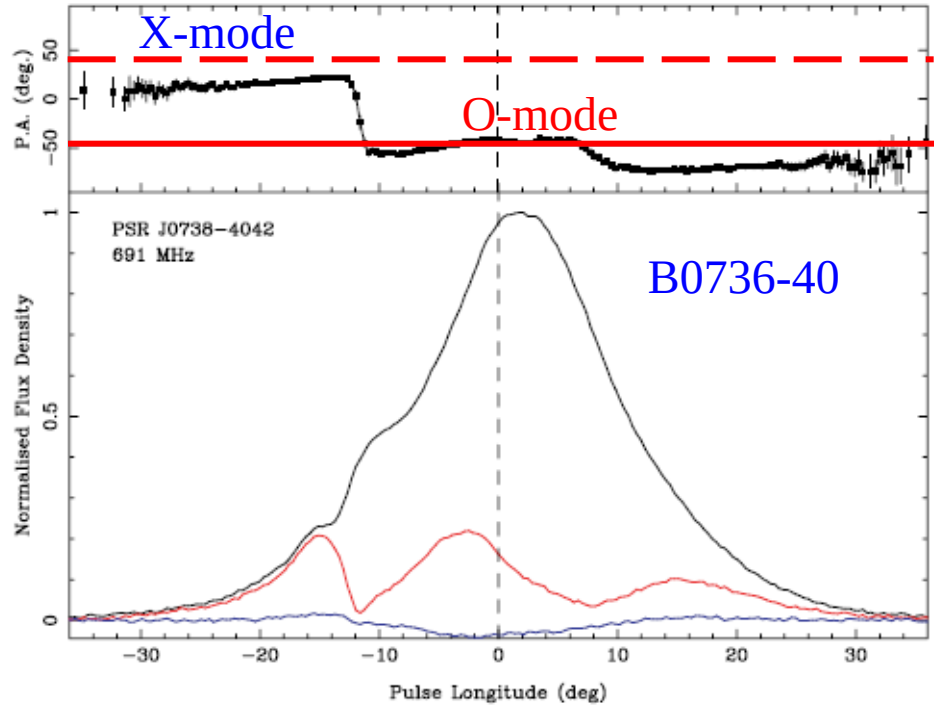

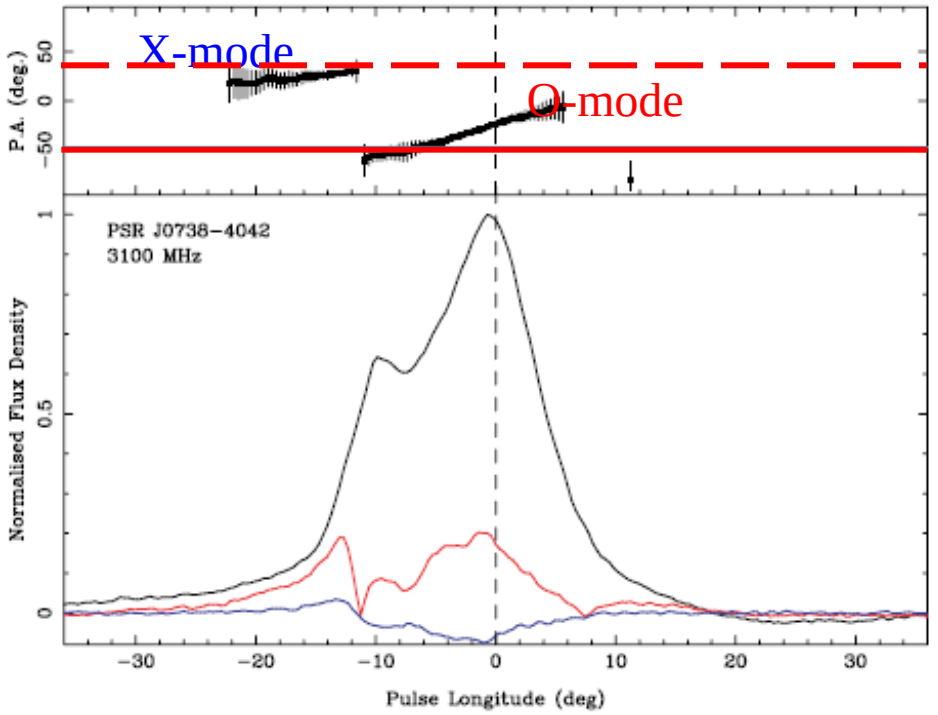

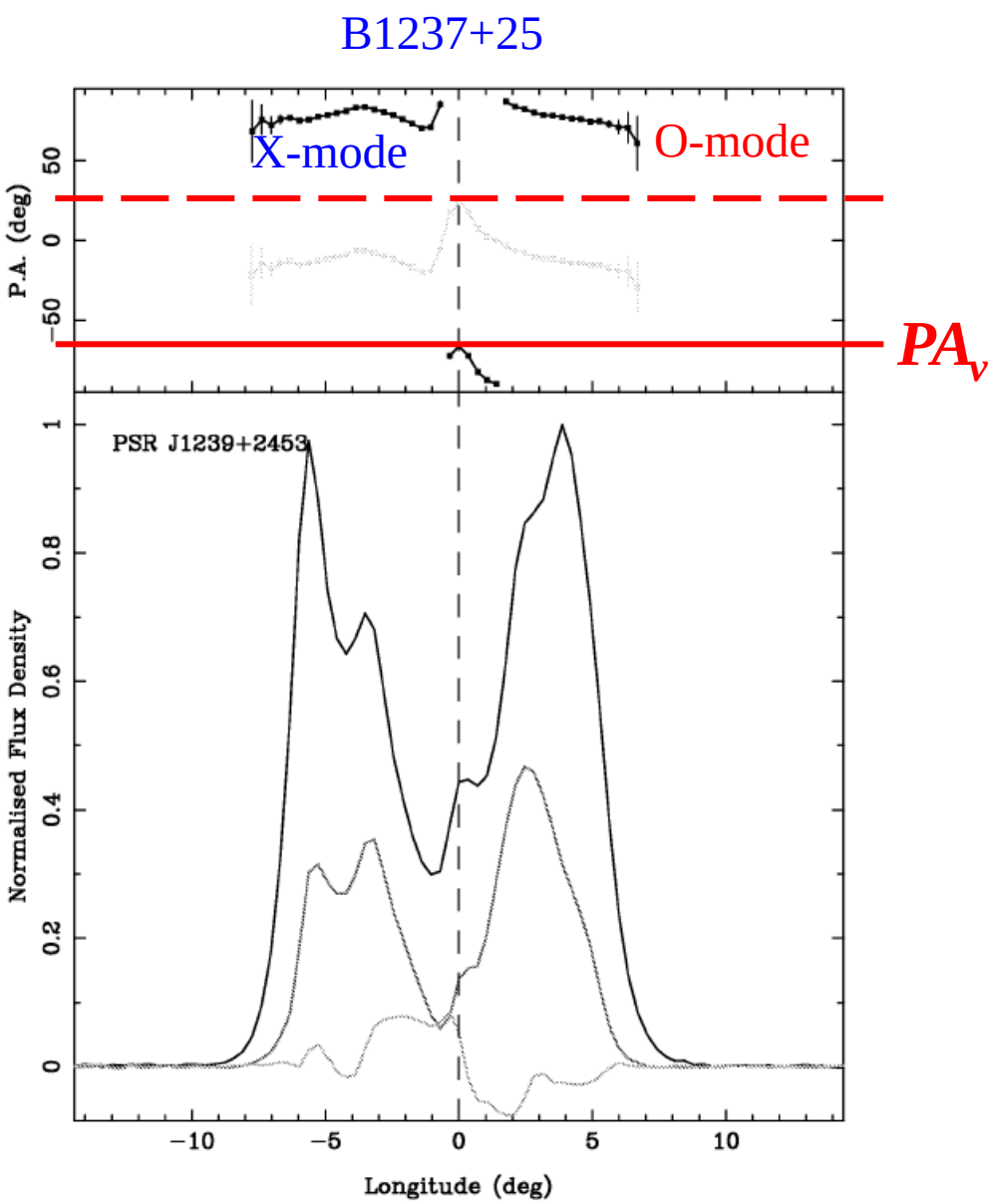
B1237+25
X-mode
O-mode
PA_v
P.A. (deg)
PSR J1239+2453
Normalised Flux Density
Longitude (deg)

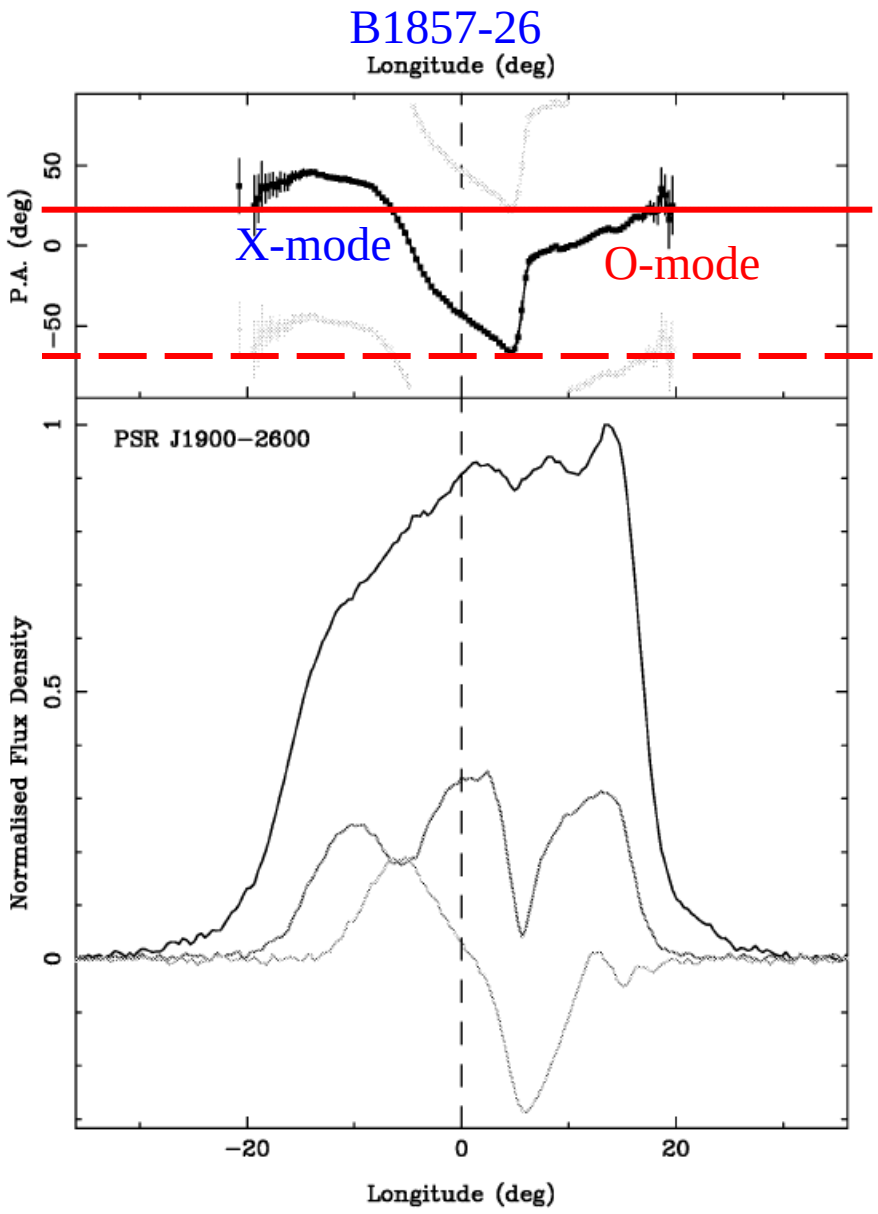
B1857-26
Longitude (deg)
X-mode
O-mode
P.A. (deg)
PSR J1900−2600
Normalised Flux Density
Longitude (deg)

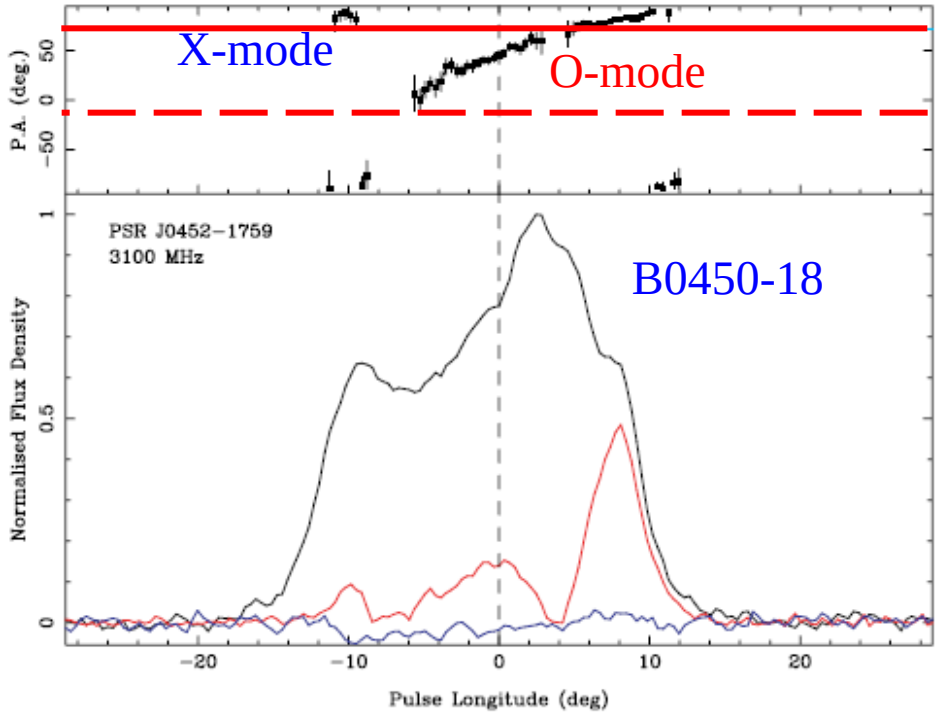
X-mode
O-mode
P.A. (deg.)
PSR J0452−1759
3100 MHz
B0450-18
Normalised Flux Density
Pulse Longitude (deg)

PA_v

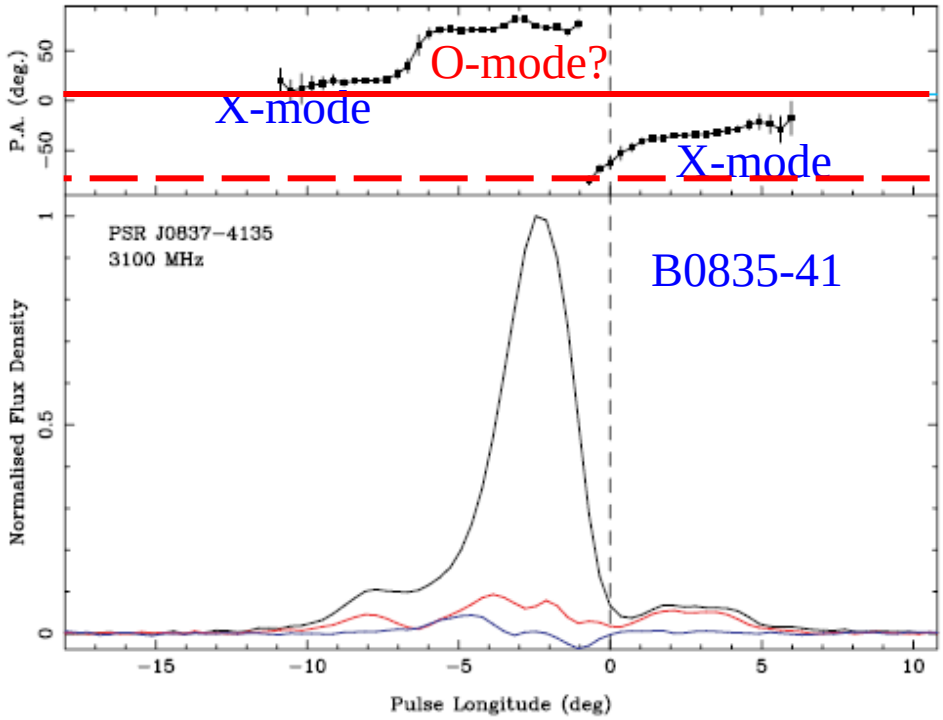
O-mode?
X-mode
X-mode
P.A. (deg.)
PSR J0837−4135
3100 MHz
B0835-41
Normalised Flux Density
Pulse Longitude (deg)

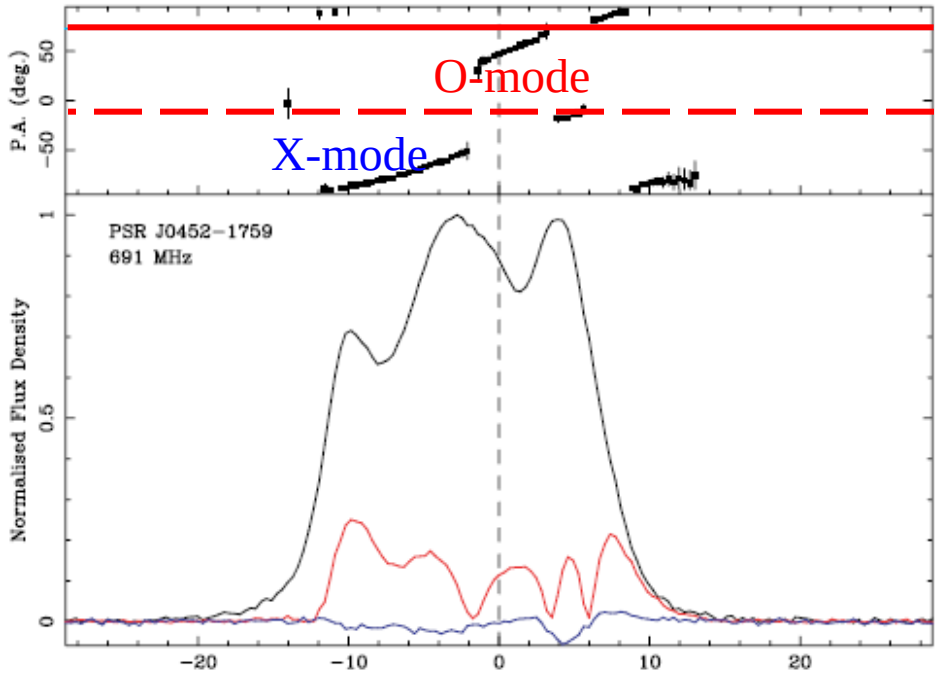
O-mode
X-mode
P.A. (deg.)
PSR J0452−1759
691 MHz
Normalised Flux Density

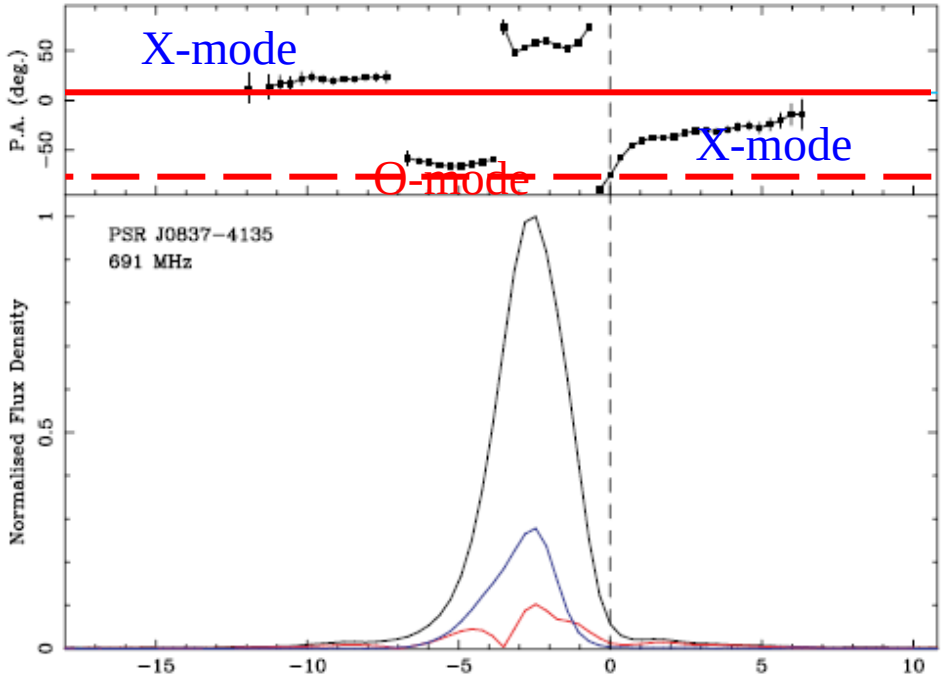
X-mode
X-mode
O-mode
P.A. (deg.)
PSR J0837−4135
691 MHz
Normalised Flux Density

B0355+54

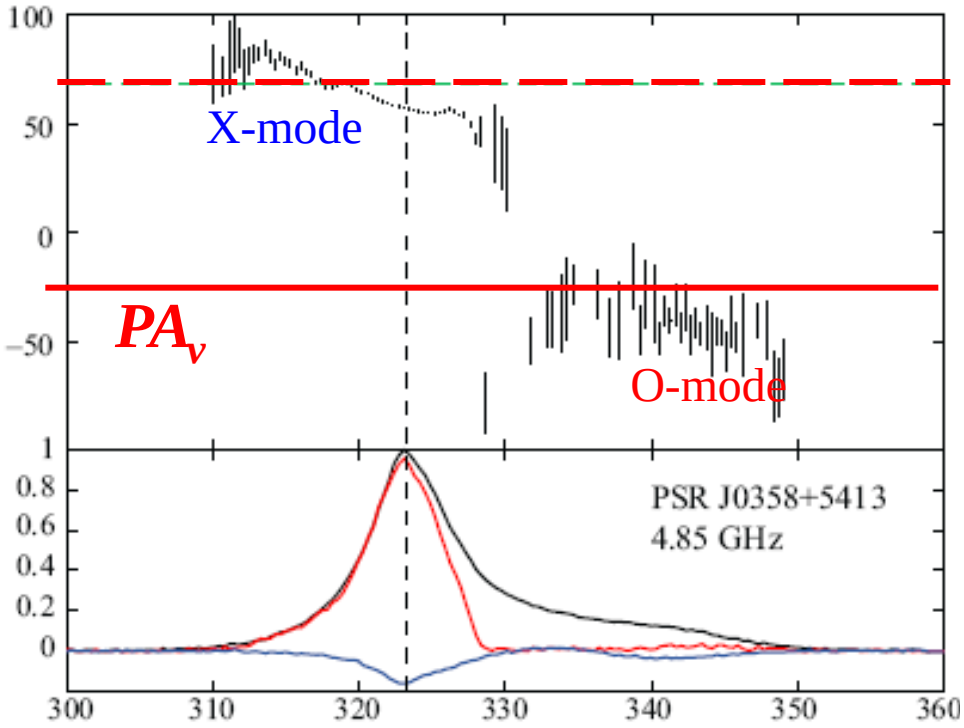

J1735-0724

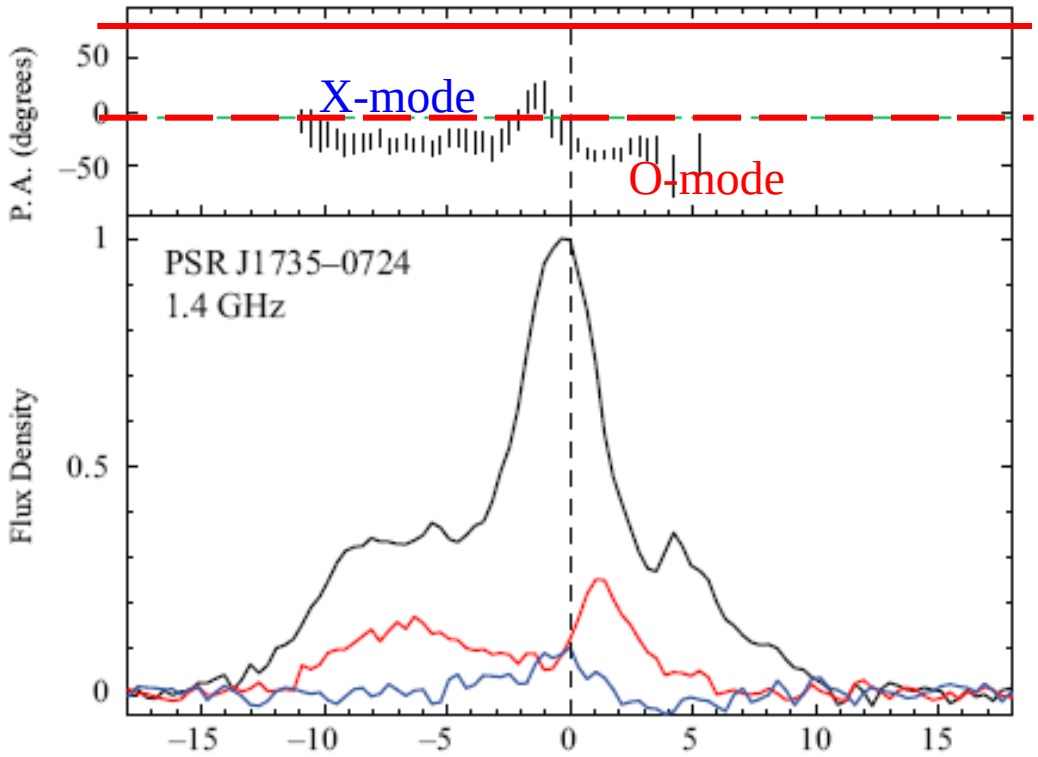

8颗脉冲星 X-mode位于leading side

J1453-6413

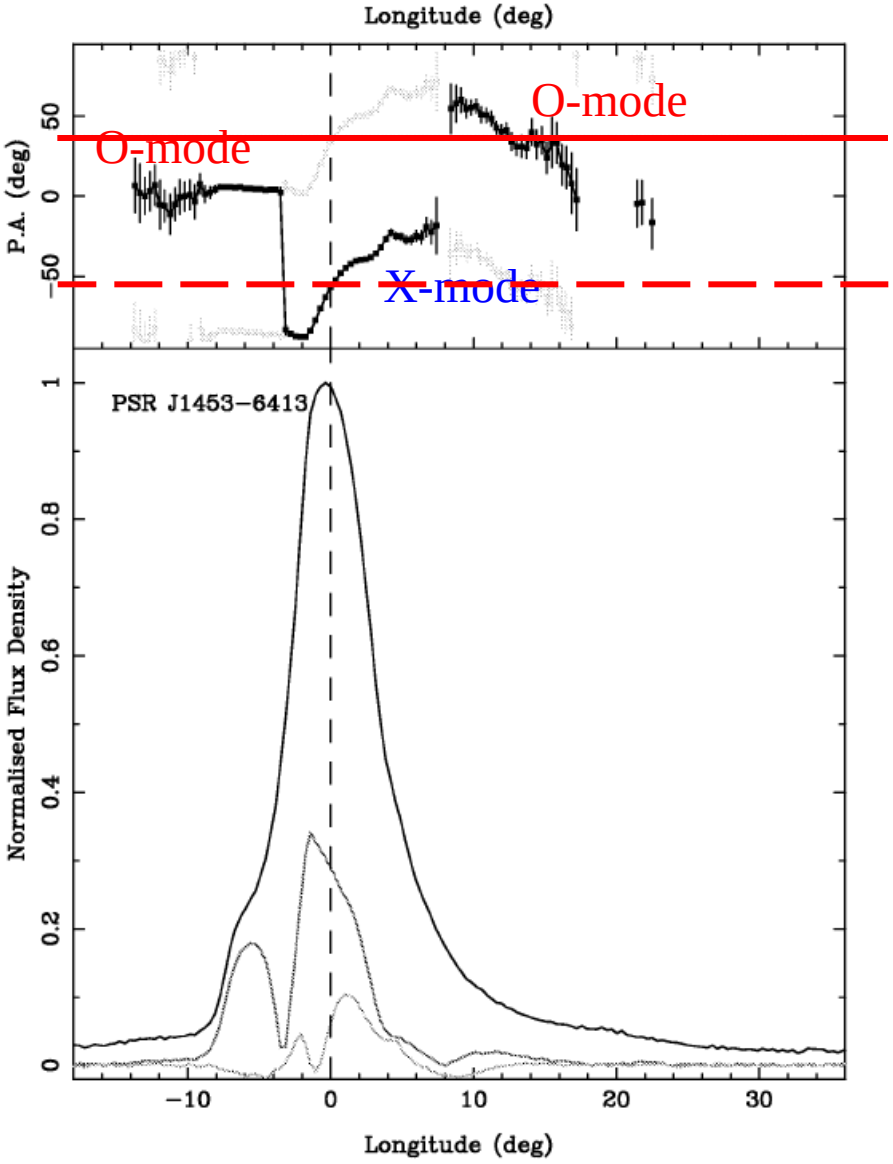

PA_v

J0953+0755

X-mode

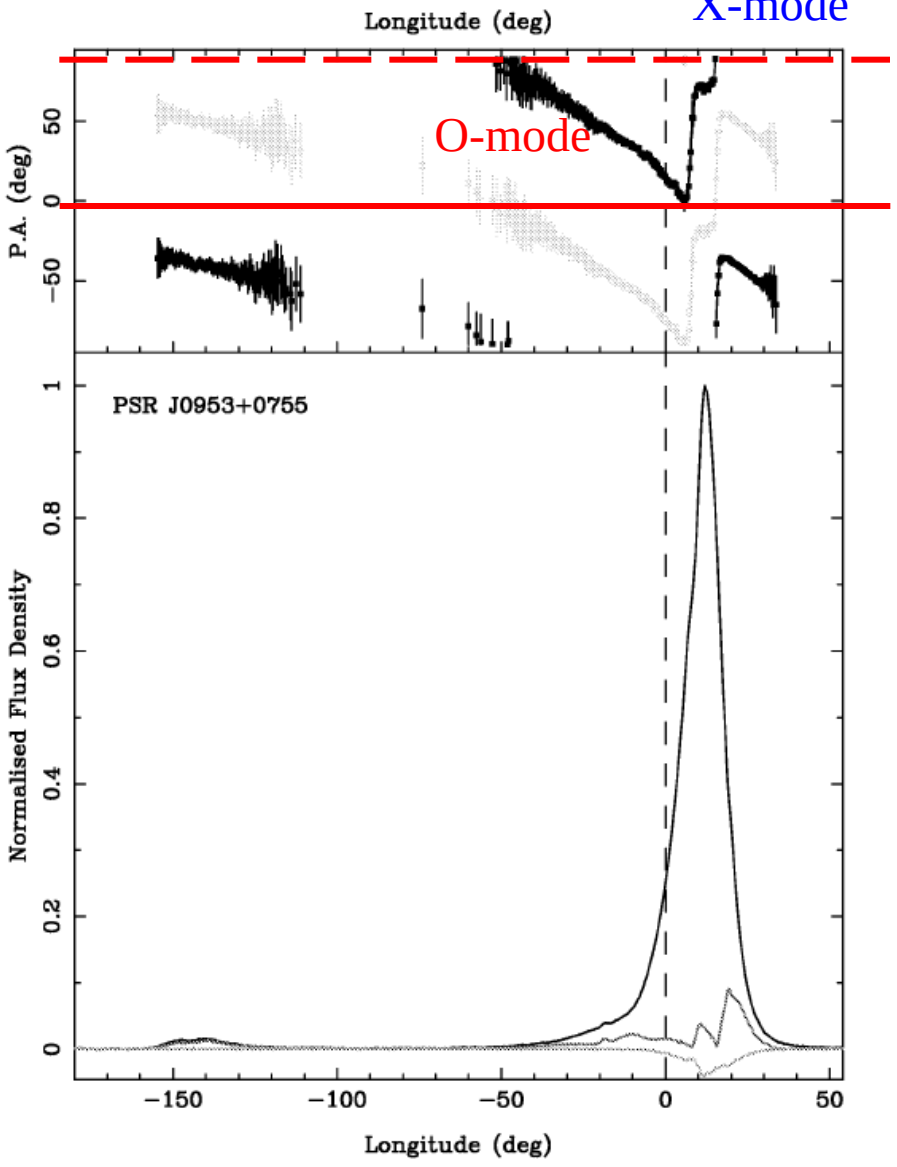

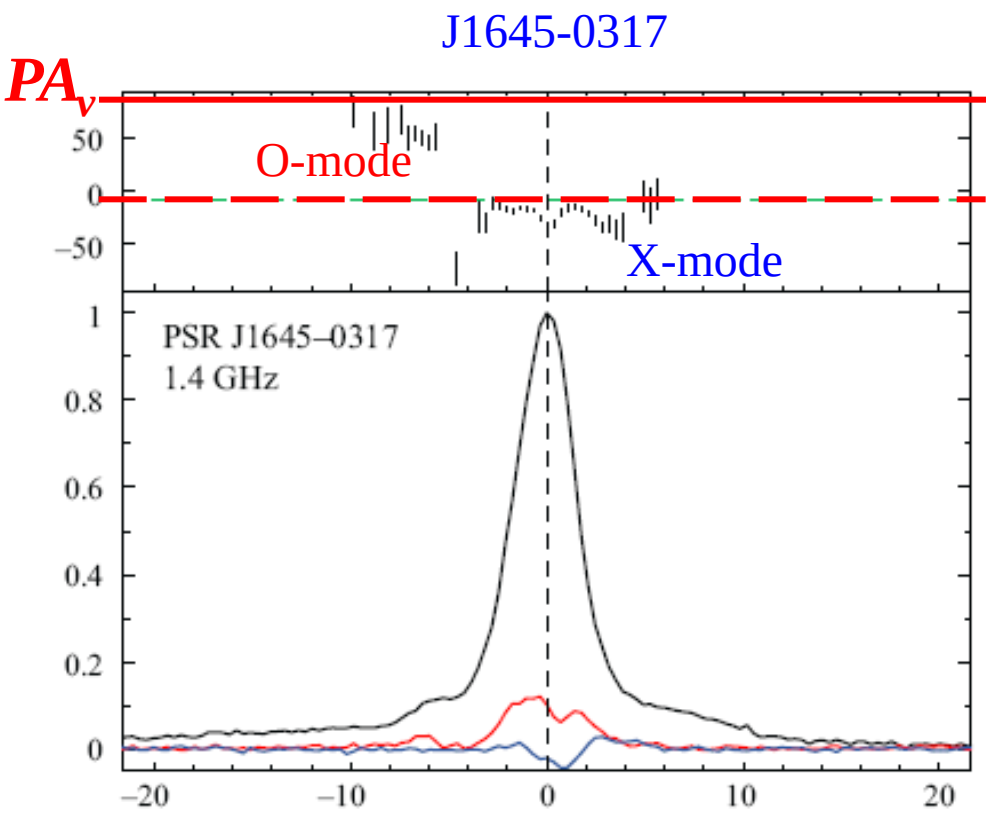

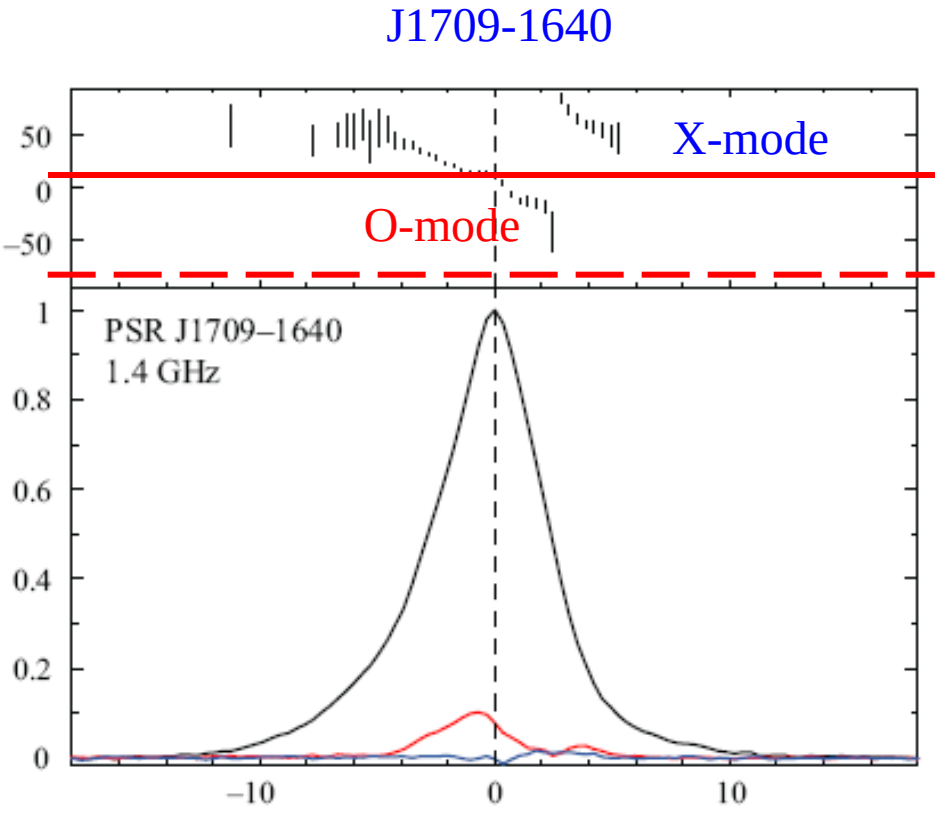

4颗脉冲星 O-mode位于leading side

8颗脉冲星 X-mode位于leading side

Conal-Double PSRs 中PA与V的关系

- Conal-double pulsars,

PA increase → V < 0

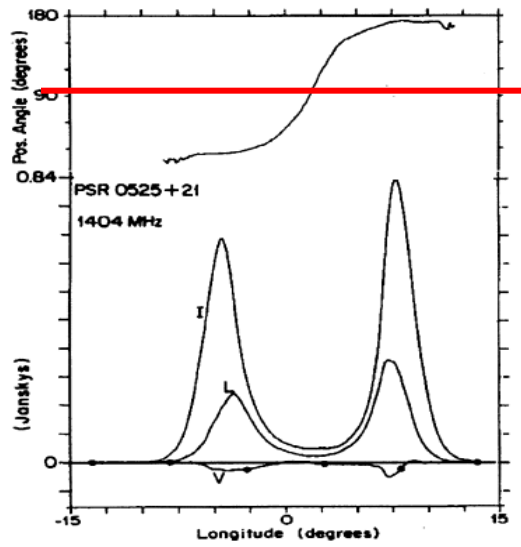

PA*v*

PA decrease → V > 0

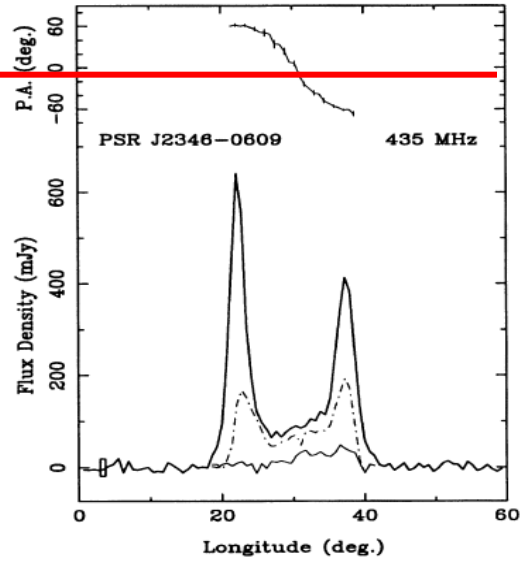

Han et al. 1998,
You et al. 2006

可以利用磁层中的波模耦合传播效应来很好的解释

波模耦合产生的圆偏振
依赖于PA的变化趋势

$$V/I = 2.2\mathrm{sign}(\phi'_B)|r_{\rm pl}\phi'^{3}_{B}|^{3/2}$$

$$\phi'_B \simeq \frac{\mathrm{d}\phi_{\rm PA}}{\mathrm{d}\Psi}\frac{1}{r_{\rm LC}}$$

要求：Conal-Double PSRs的偏振辐射都是O-mode！

可以用PA_{0v}来检验是否为O-mode

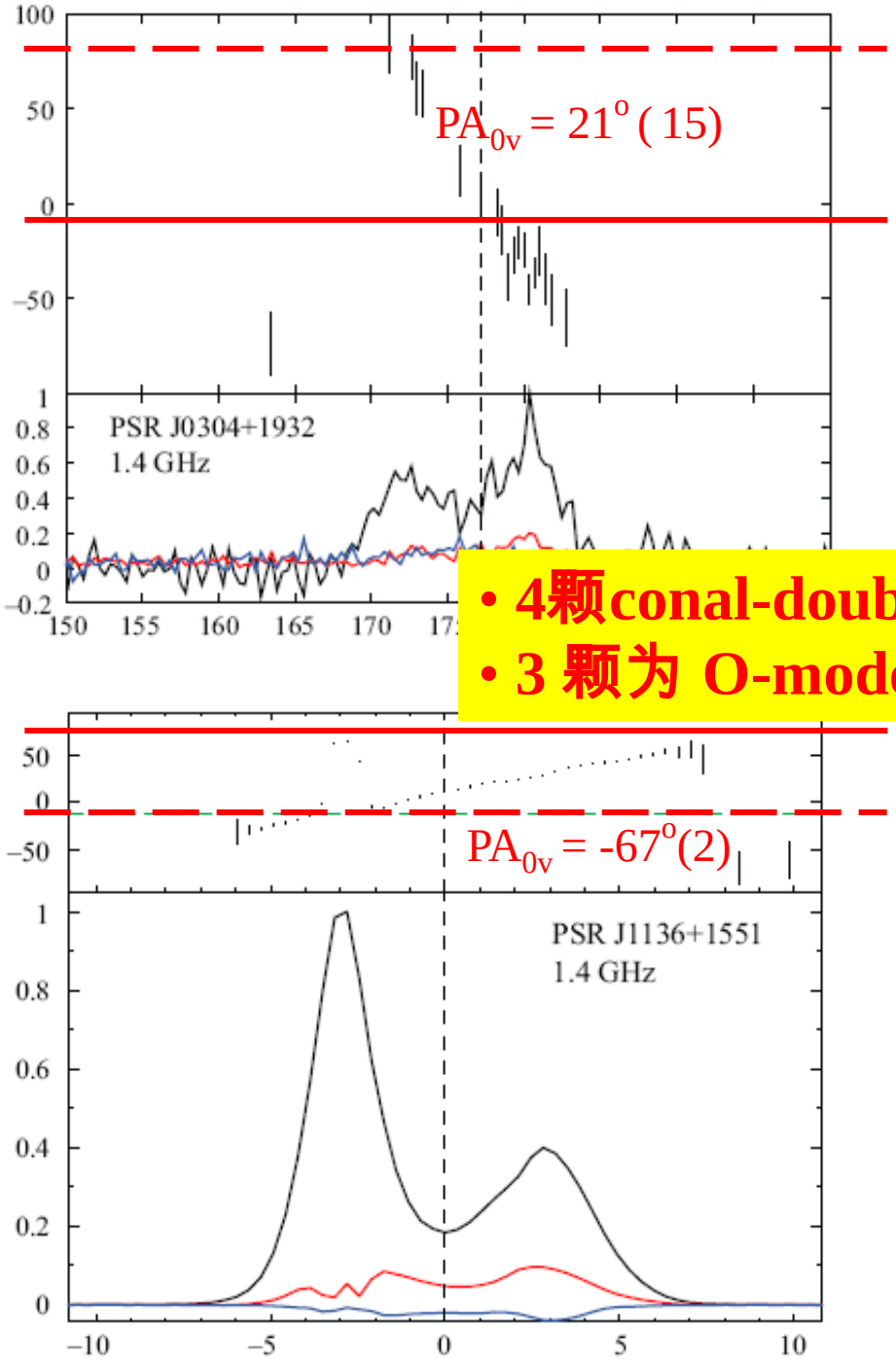

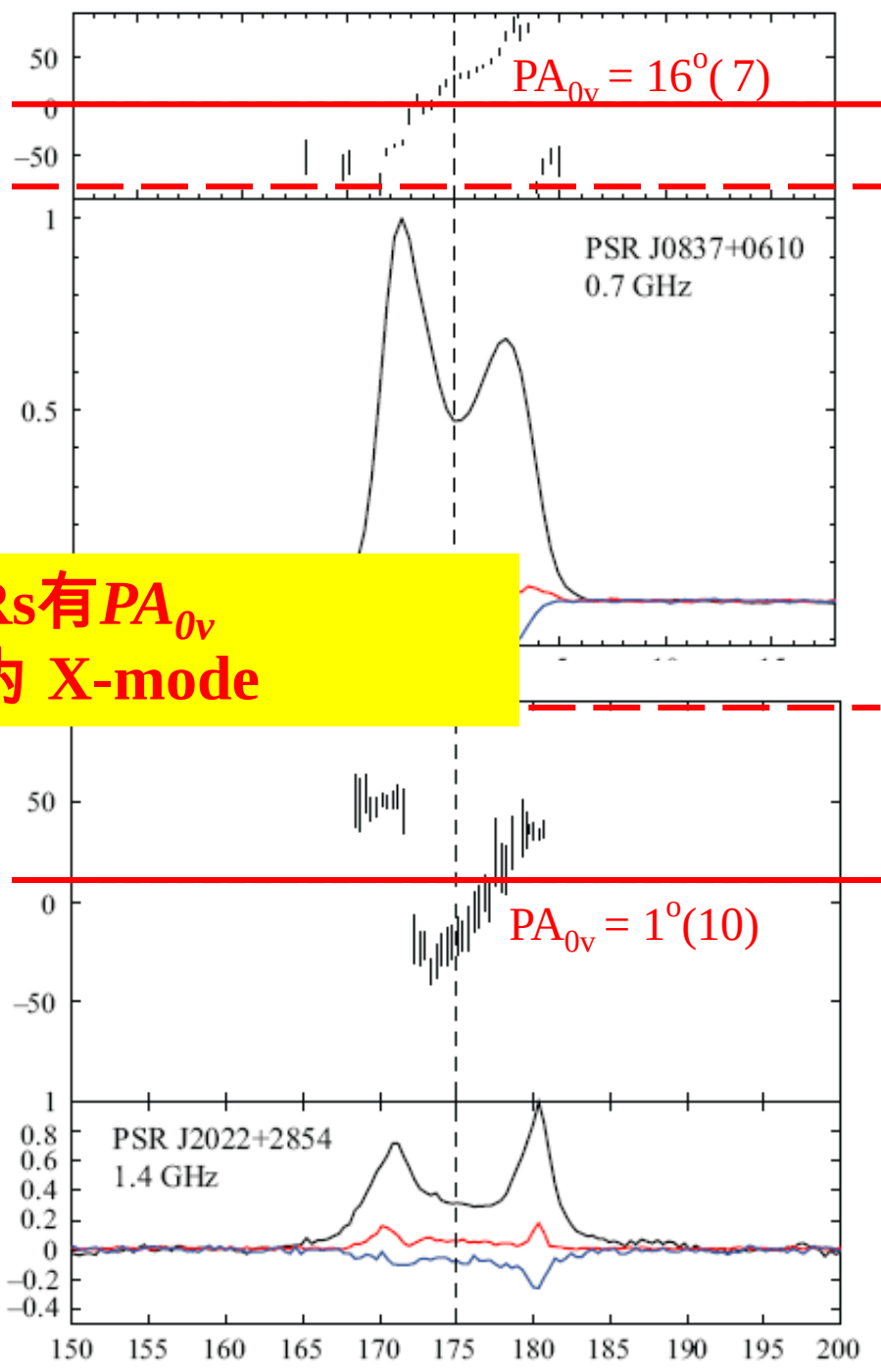

- **4颗conal-double PSRs有PA_{0v}**
- **3 颗为 O-mode, 1颗为 X-mode**